2014

INTERPRETATION OF SHALLOW HELICAL ANCHOR CAPACITY IN SAND

Joseph Robert Giampa
University of Rhode Island, giampaj@gmail.com

INTERPRETATION OF SHALLOW HELICAL ANCHOR CAPACITY IN SAND

BY

JOSEPH ROBERT GIAMPA

A THESIS SUBMITTED IN PARTIAL FULFILLMENT OF THE

REQUIREMENTS FOR THE DEGREE OF

MASTER OF SCIENCE

IN

CIVIL AND ENVIRONMENTAL ENGINEERING

UNIVERSITY OF RHODE ISLAND

2014

MASTER OF SCIENCE THESIS

OF

JOSEPH ROBERT GIAMPA

APPROVED:

Thesis Committee:

Major Professor Aaron S. Bradshaw

Christopher D.P. Baxter

David G. Taggart

Nasser H. Zawia

DEAN OF THE GRADUATE SCHOOL

UNIVERSITY OF RHODE ISLAND
2014

ABSTRACT

This thesis presents a comparison between measured breakout capacity and a range of theoretical capacity solutions (i.e. limit equilibrium, limit analysis, finite element and cavity expansion) for shallow embedded anchors in sand. Evaluation and reviews are performed using a database of measured vertical breakout capacity results from large-scale, shallow embedded, single-helix anchors collected by the author. Understanding the soil-anchor interaction and predicting the capacity of shallow circular plate and helical anchors in sands has been a major focus among geotechnical engineering researchers since the 1950's. A number of models have been developed which range from purely theoretical to semi-empircal and empirical formulations. There is uncertainty in the current models due to limitations in theory and experimental data used for validation. Attention in most models is focused on the shape and size of the failure surface and lateral earth pressures established during anchor uplift; the components affect shear stresses and the weight of soil being displaced, thus the total breakout capacity. The identified theoretical models were evaluated using the soil properties measured and estimated from the large-scale test results that were performed. Results suggest an over-prediction in capacity among many of the limit equilibrium models, with the exception of a re-derived limit equilibrium model that considers non-associated flow. Furthermore, good agreement is seen between the finite element and cavity expansion models as well as some limit analysis methods.

ACKNOWLEDGMENTS

This thesis would not have been possible without my Major Professor, Dr. Aaron Bradshaw, for his support, inspiration, and pure enthusiasm throughout my research and academic career. For this I would like to express my genuine appreciation. I am truly grateful for all of the opportunities you have provided me during both my undergraduate and graduate studies. In addition, thank you for your commitment to provide me with funding for my education, as well as your constant motivation, ideas, and friendship.

In addition, I would like to thank Dr. James A. Schneider for his input and assistance toward my research. I would further like to extend my appreciation out to Dr. Christopher Baxter for providing me knowledge and insight throughout my graduate studies.

I am extremely and without a doubt grateful to Kara Clement for always being there for me and giving me her tremendous love, encouragement, and motivation to continue forward and grow. Thank you and I love you with all my heart.

A special thanks goes out to my friends and colleagues, Jeff Costa, Amanda Costa, Alesandra Morales, Mike Dobling, and Fabian Dietrich for their friendship, supportiveness, and help throughout my research. I would also like to thank Kevin Broccolo for assisting throughout my research.

Finally, I would like to thank my wonderful and supportive parents, Joann and Stephen. You have always been there and helped me strive to be the best I can be and have given me encouragement in every aspect of my life. Thank you for providing me with an amazing education and your unconditional support. Thank you so much for your genuine interest in my work and for always being there and supporting me throughout my entire life, if it was not you I would not be the person I am today. Thank you Mom and Dad.

PREFACE

Manuscript format is in use throughout this thesis. This thesis is comprised of one manuscript with the intent of future publication in a scholarly journal. The manuscript will discuss multiple theoretical interpretation methods to predict the ultimate breakout capacity of shallow, single-helix anchors embedded in sand. A review of the models will be presented and compared directly to large-scale experimental data gathered by the author.

TABLE OF CONTENTS

LIST OF TABLES

LIST OF FIGURES

MANUSCRIPT

Interpretation of Shallow Helical Anchor Capacity in Sand

By

Joseph Robert Giampa

ABSTRACT

This thesis presents a comparison between measured breakout capacity and a range of theoretical capacity solutions (i.e. limit equilibrium, limit analysis, finite element and cavity expansion) for shallow embedded anchors in sand. Evaluation and reviews are performed using a database of measured vertical breakout capacity results from large-scale, shallow embedded, single-helix anchors collected by the author. Understanding the soil-anchor interaction and predicting the capacity of shallow circular plate and helical anchors in sands has been a major focus among geotechnical engineering researchers since the 1950's. A number of models have been developed which range from purely theoretical to semi-empircal and empirical formulations. There is uncertainty in the current models due to limitations in theory and experimental data used for validation. Attention in most models is focused on the shape and size of the failure surface and lateral earth pressures established during anchor uplift; the components affect shear stresses and the weight of soil being displaced, thus the total breakout capacity. The identified theoretical models were evaluated using the soil properties measured and estimated from the large-scale test results that were performed. Results suggest an over-prediction in capacity among many of the limit equilibrium models, with the exception of a re-derived limit equilibrium model that considers non-associated flow. Furthermore, good agreement is seen between the finite element and cavity expansion models as well as some limit analysis methods.

INTRODUCTION

The helical anchor is an earth anchor constructed of a steel helix that gets rotated into the soil like a screw. The anchor consists of a helical-shaped circular steel plate welded to a steel circular or square shaft at a given spacing. Typical configurations are shown in Figure 1. Through the use of truck mounted, trailer mounted, or handheld equipment, helical anchors can be rotated into the ground (Mitsch & Clemence, 1985). The first recorded use of the helical anchor was in the 1830's in England as moorings and lighthouse foundation systems. Alexander Mitchell, a brick maker and civil engineer, puzzled over the issue to better foundation marine structures on weak soils. The outcome was the develpoment of the helical anchor (Lutenegger, 2011). The helical anchor can be used in applications where resistance against tension and compression loading is needed (Saeedy, 1987). These anchors are cost effective due to the minimal construction equipment and energy nessessary for installation. The recycling of these foundations is also possible particularly in the oil and gas industry where temporary anchorage is necessary for floating structures. Other applications of helical anchors include: foundation systems for homes, commerical buildings, light poles, transmission towers, retaining walls, and as underpinning elements for failed foundations or to extend existing foundations to handle additional loads (Perko, 2009).

Helical anchors generate capacity through bearing on the helix plate against the soil as well as the weight and friction due to the soil wedge created during uplift. Single-helix or multi-helix anchors are commonly found in practice; a typical design of a multi-helix anchor is shown in Figure 2, and consists of a tapered point with helical bearing

plates located above. Each bearing plate is fabricated at a pitch to allow the cutting of soil during installation; this allows the anchor to progress into the ground with ease. The capacities of helical anchors are primarily dependent on the helix diameter, embedment depth, soil density, and spacing of helicies.

Understanding the soil-anchor interaction and predicting the capacity of shallow circular plate and helical anchors in sands has been a major focus among geotechnical engineering researchers since the 1950's. A number of models have been developed to predict anchor capacity, which range from purely theoretical to semi-empircal and empirical formulations. These models cover a range of embedment ratios from approximately D/B = 1 to 10, where B is the diameter of the anchor and D is the embedment depth. There is uncertainty in the current models due to limitations in theory and experimental data used for validation. The semi-empirical and empirical models are constrained by specific soil conditions and anchor geometry. This thesis will be focused on a range of theoretical breakout capacity models for shallow embedded anchors in sand. All analyses are considered to be drained in sand, where an effective stress analysis is used.

The objective of this thesis will be to evaluate the identified theoretical breakout capacity models for shallow, circular plate and single-helix anchors in sands. Evaluation and review will be made using shallow embedded, large-scale, single-helix anchor breakout test results collected by the author. The subsequent sections will include a review of the identified theoretical capacity models found in the literature, a

limit equilibrium capacity model adapted from White et al. (2008) re-derived for helical anchors, the experimental program, and results and conclusions.

THEORETICAL ANCHOR CAPACITY MODELS

The ultimate breakout capacity relationship of anchors has been developed through theoretical approaches such as upper and lower bound limit analysis, limit equilibrium, and finite element modeling. Other predictive models have been developed using similar approaches but can be classified as semi-empirical and empirical; among these models are, Mitsch & Clemence (1985), Ghaly & Hanna (1991), Ghaly (1995), Ghaly & Clemence (1998), and Ilampurthi et al. (2002). Other models that have not been presented include Balla (1961), Baker & Konder (1966), and Andreadis et al. (1981), because these models are limited to specific soil and anchor conditions. Therefore only identified theoretical capacity models for shallow embedded, circular or helical anchors will be considered in this thesis as to avoid such constraints.

The development of many of the capacity relationships typically begins with an assumed or observed failure surface and stress distribution (which will vary from shallow to deep embedment). Figure 3 shows various assumed and/or observed failure surfaces found in the literature. Equation 1 describes the ultimate pullout force, Q_u, as a function of the overburden stress, $\gamma'D$, the area of the anchor, A, and an anchor capacity factor, $N\gamma$. Table 1 provides a summary of the identified theoretical models and how they describe $N\gamma$:

$$Q_u = N_\gamma \gamma' DA \qquad (1)$$

Limit analysis approaches are used to bracket the true collapse loads (i.e. breakout capacity) from above and below. Upper and lower bounds are created assuming that the soil behaves as a perfectly plastic material obeying an associated flow rule, assuming that $\phi' = \psi$, where ϕ' is the friction angle and ψ is the dilatancy angle of the soil. Lower bound solutions represent the condition in which applied loads do not cause yielding or failure to a body; in soil mechanics this bound is termed a safe solution because if an error is made and higher loads are applied, the body (i.e. soil mass) should be able to tolerate the new loads without violating its failure criterion. The major assumption is that if the internal stresses in a soil mass are in equilibrium with external loads, including self-weight, and in nowhere reaches the failure criterion or yields, a lower bound can be defined. Through iteration, typically the highest lower bound is found and is still below the true collapse load.

Alternatively, upper bound solutions are developed and termed unsafe solutions as a lower load may cause collapse. If a mechanism can be found such that the work done by any external loads and body forces equals the amount of energy dissipated in the soil mass during deformation, then an upper bound is found. Similarly, through iteration a least upper bound solution is searched for such that it exceeds the true collapse loads (Powrie, 2004; Yu, Salgado, & Sloan, 1998). However, by equating a lower and upper bound an exact solution can be found.

Alternatively, limit equilibrium solutions are used to estimate an exact solution rather than a bound as limit analysis does. In contrast, limit equilibrium assumes a failure

surface and the forces acting on that surface are determined. Typically, the failure surface is assumed to be a surface inclined at an angle, θ and the Mohr-Coulomb failure criterion is applied to that surface where the shear stress and normal force are unknown. A valid solution requires equilibrium compatibility and the stress-strain relationship to be satisfied (Chen & Scawthorn, 1968). Many of the theoretical capacity models are developed using the abovementioned theories, as well as through more sophisticated approaches such as finite element modeling and cavity expansion theory. The following theoretical investigations will be divided into subcategories of limit equilibrium, limit analysis, and additional methods.

Limit Equilibrium

Meyerhof & Adams (1968) proposed a theoretical relationship to predict pullout capacity of horizontal, strip and rectangular anchors. The authors' limit equilibrium solution assumed that the failure surface was inclined at the plate edge that reaches the ground surface during uplift at shallow depths (Figure 3b). The average angle of the failure surface with the vertical, for sands, was stated to be $\frac{\phi'}{3}$, where ϕ' is the friction angle. The solution was derived for a strip and continuous footing and then modified for sands and clays for circular and rectangular footings (Meyerhof & Adams, 1968). The author's further state that uplift is governed by the vertical component of passive pressures, K_{pv}. The ultimate pullout capacity was determined by considering equilibrium of the material between the anchor and the soil surface. Meyerhof & Adams (1968) extended the analysis of shallow strip footings to circular anchors by

using a theoretical shape factor that governs the passive earth pressure on a convex cylindrical wall.

Meyerhof & Adams (1968) validated their solution using small-scale models at shallow and deep embedment along with shallow, full-scale pullout tests performed by Ontario Hyrdro. The diameter of the model tests ranged from 25 mm to 102 mm and the diameter of the full-scale tests was 76 mm. Further comparisons were made using full-scale test results reported in the literature. The comparison between the theory and the test results showed good predictions at great depths and under-predicted at shallow depths.

The limit equilibrium model presented by Murray & Geddes (1987) was developed assuming a failure surface that begins vertical at the plate edge and curves as it approaches the ground surface (Figure 3c). The failure surface meets the vertical at an angle of $\frac{\phi'}{2}$. The author's assume K_o conditions to estimate the lateral earth pressures acting along the failure surface created during uplift. Laboratory test results were presented in conjunction with the equilibrium methods developed by the authors, along with existing theoretical solutions found in the literature. The model tests were carried out using 51 mm and 89 mm rectangular and circular plate anchors over a range of embedment ratios (D/B) between 1 and 10. The equilibrium solution developed by Murray & Geddes (1973) and existing theories in the literature compared satisfactorily with the small-scale experimental results; however the trend among the solutions was an over-prediction of capacity.

Saeedy (1987) has developed a dimensionless design chart to estimate the breakout capacity for circular earth anchors. The solution was formulated by initially considering the system at a state of rest; then when subjected to a vertical pull, the soil above the anchor compresses. The amount of compression caused by the anchor depends on the original state of the soil, thus as the process continues the shear stress level reaches the shear strength of the soil, creating a shear failure surface that develops progressively as the external load increases. Saeedy assumes this failure surface to take a log spiral form. The failure surface (Figure 3c) begins vertical at the plate edge and meets the ground surface at an angle of $45-\frac{\phi'}{2}$. A differential equation describing the complex shear stress distribution treats a differential element under equilibrium along an assumed failure surface known as the Kotter equation. Lateral earth pressures are further defined to equal the vertical effective stress. Saeedy (1987) compared his solution to a range of experimental results from a 76 mm diameter anchor obtained from Saeedy (1971). Other experimental comparisons were made using field and model tests. The theoretical model showed good agreement between both the experimental and field results.

Sarac (1989) presents a limit equilibrium solution for circular anchor slabs in the form of a design chart. The dimensionless breakout factor can be selected as a function of friction angle and embedment ratio. To solve the limit equilibrium solution the author implemented the method of finite differences. A log spiral failure surface (Figure 3c) was assumed by the author inclined at the plate edge, which met the ground surface at an angle of $45-\frac{\phi'}{2}$. To account for the presence of lateral earth pressures along the

failure surface, Sarac utilized a theory of complete limit equilibrium for axially symmetrical problems developed by V.G. Berezancev by means of a differential equation found in Sarac (1989). Sarac's theoretical solution was compared against his own model tests in two kinds of sand and with model tests found in the literature. The results were found to be in excellent agreement, which confirmed that the capacity was expressed properly in terms of embedment ratio (D/B) and friction angle.

Ghaly & Hanna (1994) developed a theoretical breakout relationship for single-helix screw anchors using limit equilibrium with an observed log spiral failure surface inclined at the plate edge. The failure surface (Figure 3c) is assumed to reach the ground surface at an angle $45-\frac{\phi'}{2}$. Lateral earth pressures were estimated assuming a passive earth pressure coefficient, K_p. The solution was a function of friction angle, soil density, and embedment ratio. Weight and shear factors for shallow and deep anchors were developed for simplification to determine pullout capacity. Ghaly & Hanna (1994) compared the solution with single-and-multi-helix screw anchors reported in the literature. The anchor diameter used to develop the limit equilibrium solution was 343 mm. Both the experimental results performed, and found in the literature showed good agreement to the author's theoretical solution.

Hanna et al. (2007) presented analytical models to predict the breakout capacity and load-displacement relationship for shallow single-helix and plate anchors in sand. The models were formulated using limit equilibrium and a failure surface observed through laboratory model testing presented in Ghaly and Hanna (1991). It was assumed that the failure surface is inclined at the plate edge and the angle of inclination varies based

on geometry. Empirical expressions are presented to determine the critical depth (to separate shallow from deep anchors) and the radius of influence on the ground surface. Furthermore, values of passive earth pressures were assumed in the theoretical model. The authors used existing theories and experimental results found in the literature for comparisons. Their model showed good agreement with the experimental and field results for single-helix and plate anchors in loose and medium-dense sand, however differences were found between the predicted and measured in dense sands, which believed to be due to the dilatancy effect at shallow depths.

Limit Analysis

Murray & Geddes (1987) utilized upper and lower bound limit analysis to estimate breakout capacity of circular plate anchors. The upper bound limit analysis approach showed that the failure surface extends to the ground surface at an angle of ϕ' at the plate edge (Murray & Geddes, 1987). The lower bound formulation is defined as the weight of soil vertically above the anchor plate. Combining both analyses a capacity envelope can be predicted. Laboratory model tests performed on circular anchors with diameters of 51 mm and 89 mm were compared with the authors' theoretical models. Consistent with the theory, the author's upper bound solution over-predicted capacity, and proved to be a better correlation than their previously developed limit equilibrium solution.

Merifield et al. (2006) applied a three-dimensional, numerical lower bound limit analysis and axisymmetric displacement finite element analysis to evaluate the shape of the anchor during pullout and its effect on capacity. Similar to the other proposed

models, dimensionless breakout factors were formulated for circular and rectangular plate anchors. The author's formulation was based upon associated flow assuming $\phi' = \psi$, where ψ is the angle of dilatancy. Merifield et al. (2006) used numerical and empirical solutions presented in the literature for comparison, which included Balla (1961), Meyerhof & Adams (1968), Murray & Geddes (1987), Sarac (1989), Saeedy (1987), Ghaly & Hanna (1994), and Ilamparuthi et al. (2002). The authors found that the lower bound solution compared well with axisymmetric displacement finite element results but were less favorable against the range of theoretical solutions found in the literature.

Additional Methods

Rowe & Davis (1982) present theoretical influence charts for the use in hand calculations to estimate anchor breakout capacity. The author's solution can be used over a range of anchor geometry and soil types. Elasto-plastic finite element analyses were utilized to develop the model. This approach allows for the consideration of a plastic failure within the soil, anchor breakaway from the soil behind the anchor, and shear failure at a frictional, dilatant soil-structure interface. The anchor was assumed to be thin and perfectly rigid and that the soil will follow the Mohr-Coulomb failure criterion or either an associated ($\phi' = \psi$) or non-associated flow rule ($\psi < \phi'$). The initial form of the solution assumed plastic deformation at constant volume and a coefficient of lateral earth pressure at-rest equal to 1. Correction factors were further introduced to incorporate the effects of dilatancy, anchor roughness, and initial stress state. Rowe & Davis (1982) performed small-scale pullout tests on anchors of

diameter 51 mm at embedment ratios ranging from 1 to 8.75 and compared with their proposed theory. In addition, results obtained by Das & Seeley (1975) on rectangular anchors were used for validation. The comparisons indicate good agreement between the theory and experimental results.

Vesic (1971) proposed a theoretical model using close-surface cavity expansion theory described in Vesic (1965). The author presents analytical solutions for the problem of expansion of cavities close to the surface assuming a semi-infinite, rigid-plastic solid. The solutions give the ultimate radial pressure needed to break out a cylindrical or a spherical cavity at depth (Vesic, 1971). Vesic (1971) presents a table of breakout factors for cylindrical plates as a function of friction angle and embedment ratio. Through observation and theoretical consideration, the author states that the failure zone caused by a cylindrical plate should meet the surface at an angle of approximately $45-\frac{\phi'}{2}$ for shallow anchors in dense sand; for shallow anchors in loose sand the failure surface is closer to being a vertical cylinder around the perimeter of the anchor. Large-scale experimental results in literature were used to validate the theoretical model presented by the author. The expected trend of increase in breakout capacity with depth is apparent, however the magnitude does not generally agree with the theory. The experimental results were shown to be larger than the theoretical predictions.

Sakai & Tanaka (1998) evaluated the scale effect observed in the behavior of a shallow anchor in dense sand using a finite element (FE) analysis. In addition to the analysis, 1g model tests were performed on flat 0.5 cm thick circular steel plates with

diameters of 3 cm, 5 cm, 10 cm, and 20 cm at embedment ratios from 1 to 3. The FE analysis used an elasto-plastic model with a non-associated flow, strain hardening/softening law. Toyoura sand was used to develop the finite element model and does not explicitly state it is a limitation. The authors found an excellent correlation between the predictive model and 1g scale tests.

As it can be seen through the extensive literature on circular plate and helical anchors in sand, the breakout capacity has been estimated through numerous theoretical approaches. Although the majority of the predictive models presented are compared with existing pullout results either in the laboratory or the field, the models are typically calibrated or validated to small-scale tests. This calibration technique can result in difficulty representing large-scale systems and stress conditions of the soil if not properly considered. The capacity of shallow anchors significantly depends on the shape of the failure surface above the anchor and shear along that surface. Many of the theoretical models have assumed the shape of the failure surface, the angle from the vertical or horizontal, and lateral pressures, which may not represent the true in-situ conditions. Therefore, these models may lead to uncertainties in the predicted capacities. These identified models will be evaluated using full-scale, carefully characterized set of load test data collected by the author.

PROPOSED NON-ASSOCIATED FLOW LIMIT EQUILIBRIUM MODEL

As part of this study, a new axisymmetric model was derived for helical anchors using non-associated flow limit equilibrium adapted by White et al. (2008). It was assumed that the failure surface is inclined at an angle equal to the dilatancy angle, ψ, of the

soil (Figure 3b). This assumption that $\theta = \psi$, is consistent with experimental observations (i.e. White et al., 2008 and Lui et al, 2012). This occurrence affects the size of the failure wedge created by the anchor and more realistically models the behavior during breakout. Therefore the breakout capacity will be equal to the weight of the soil wedge plus the resistance along the failure surface. The weight of the soil wedge (W_{wedge}), assuming a truncated cone, is defined by Equation (2):

$$W_{wedge} = \frac{1}{3}\gamma' \pi D\left[\left(\frac{B}{2} + D\tan\psi\right)^2 + \frac{1}{2}B^2 + \frac{1}{2}BD\tan\psi\right] \qquad (2)$$

It is assumed that the normal stress on the failure surface is equal to the in-situ value assumed from K_o conditions. In other words, the normal stress on the failure surface does not change throughout deformation (Figure 4). Therefore, the peak-mobilized shear stress (τ) is determined and defined by Equation 3:

$$\tau = \gamma' D\tan\phi'_{peak}\left[\frac{(1+K_o)}{2} - \frac{(1-K_o)\cos 2\psi}{2}\right] \qquad (3)$$

Through integration along the failure surface and equating the vertical forces acting on the sliding block of soil the peak breakout resistance per unit length can be calculated as Q_u:

$$\begin{aligned} Q_u &= \frac{1}{3}\pi\gamma' D\left[\left(\frac{B}{2} + D\tan\psi\right)^2 + \frac{1}{2}D^2 + \frac{1}{2}BD\tan\psi\right] \\ &+ \pi\gamma' D^2\tan\phi'_{peak}\left[\frac{(1+K_o)}{2} - \frac{(1-K_o)\cos 2\psi}{2}\right]\left[\frac{B}{2} + D\tan\psi - \frac{2}{3}D\tan\psi\right] \end{aligned} \qquad (4)$$

The breakout factor, N_γ, for the limit equilibrium equation of a circular helical anchor is expressed by the rearrangement of Equation 4 to be a function of embedment ratio (D/B) and uplift factors (F_1, F_2):

$$N_\gamma = 1 + \frac{D}{B}F_1 + \left(\frac{D}{B}\right)^2 F_2 \qquad (5)$$

$$F_1 = 2\left[\tan\psi + \left(\tan\phi'_{peak} - \tan\psi\right)C_1\right] \qquad (6)$$

$$F_2 = \frac{4}{3}\left[\tan^2\psi + \left(\tan\phi'_{peak} - \tan\psi\right)\tan\psi C_1\right] \qquad (7)$$

$$C_1 = \frac{\left(1+K_o\right)}{2} - \frac{\left(1-K_o\right)\cos 2\psi}{2} \qquad (8)$$

where; B is the anchor diameter, D is the embedment depth, F_1 and F_2 are uplift factors, K_o is the coefficient of lateral earth pressure at-rest, γ' is the buoyant unit weight, ψ is the angle of dilation, and ϕ'_{peak} is the peak friction angle.

EXPERIMENTAL PROGRAM

The author performed 30 large-scale, single-helix anchor tests at various embedment depths in dry sand. Three test beds were prepared to different unit weights and embedment ratios (D/B) that varied from 1.8 to 7.1. The anchor tests were performed using a specially design load frame in which the base of the anchor was secured to an installation device by means of a threaded connection. The pitch and rotation rates were calibrated for each anchor to minimize soil disturbance. Anchors were installed either at a constant rate of penetration equal to the pitch at the shaft, or by applying a constant downward load. The dead weights on the load frame ranged from 400 N to

2,220 N during installation. Immediately following installation, the anchor was detached from the installation device and attached to a linear actuator and pulled out at a constant rate.

Test Anchors

Pullout tests were performed on two different sizes of single-helix anchors (Figure 5). The diameters of the anchors were 152 mm and 254 mm, with a pitch at the location of the shaft of 22 mm and 38 mm, respectively. The anchors did not have a true helix and thus the pitch increased with radial distance from the shaft to a pitch of 48 mm at the perimeter of the 152 mm diameter helix and 76 mm at the perimeter of the 254 mm diameter helix. The shaft diameters were 35 mm and 44 mm for the 152 mm and 254 mm diameter anchors, respectively. The thickness of the helix plate was 6 mm for both anchors.

Characterization of Test Soil

An important part of this study was to accurately characterize the peak friction angle, ϕ_{peak}', and the dilatancy angle, ψ, at low levels of confining stress within the test trench.

Bolton (1986) presents an empirical correlation to estimate the peak friction angle and dilatancy angle as a function of the mean effective stress and relative density. Embedded in the correlation are fitting parameters Q and R shown in Equation 9 for triaxial strain:

$$\phi'_{peak} - \phi'_{crit} = 0.8\psi = m * I_D \left(Q - \ln p'\right) - R \qquad (9)$$

where; ϕ'_{peak} is the peak friction angle, ϕ'_{crit} is the critical state friction angle, ψ is the angle of dilation, m = 3 for triaxial strain, I_D is the relative density index, p' is the mean effective stress, and Q and R are fitting parameters.

The sand used in this study was uniformly graded Golden Flint sand with a D_{50} of 0.30 mm. Table 2 summarizes the soil properties. Nine consolidated drained triaxial tests were performed at a low confining stress of approximately 30 kPa; the peak friction angle, ϕ'_{peak}, was recorded for each test (Table 3). To estimate the critical state friction angle, ϕ'_{crit}, the approach presented by Salgado et al. (2000) was used for every triaxial test. Critical state is obtained when the shear stress and volume become constant with increasing shear strain. To obtain $\phi'_{crit,}$ the point on the volumetric vs. axial strain curve becomes horizontal was located; at this location the dilatancy angle is zero (Figure 6b). The value of axial strain was then matched to the stress-strain curve (Figure 6a) and the critical state friction angle was estimated (Salgado et al., 2000).

The method presented in Santamarina and Cho (2001) was further used to estimate ϕ'_{crit}. The critical state friction angle is defined as the angle of repose; by pouring soil in a graduated cylinder filled with water and then rotating it beyond 60^o and bringing it back slowly to the start position, the angle of repose can be measured in the middle region of the slope. Both Salgado et al. (2000) and Santamarina and Cho (2001)

yielded similar values of ϕ'_{crit}. Thus, it was decided to use an average critical state friction angle for Golden Flint sand of 32^o.

In this thesis the fitting parameters Q and R presented in Bolton (1986) were found through rearranging Equation 9 and performing a linear regression on the data for Golden Flint Sand as proposed by Salgado et al. (2000) (Figure 7). The best fit for Golden Flint sand gives Q = 9.64 and R = -1.56, with an exceptional coefficient of determination ($r^2 = 0.953$). Using the aforementioned fitting parameters and Equation 9 the dilatancy and peak friction angles was estimated for each helical anchor test.

Trench Preparation

Anchor testing was conducted in a reinforced concrete trench with dimensions of approximately 1.5 m x 1.5 m x 21 m and was filled with 59 metric tons of fine uniformly graded Golden Flint sand. Figure 8 presents the grain size curve for the Golden Flint sand. The sand was placed through dry pluviation. It was determined that the density was controlled by the flow of sand, angle of the dispensing tray, and fall height into the trench.

The sand pluviator (Figure 9) consisted of a frame, hopper, internal distribution drum, dispensing tray, drive wheels, and electric motor. The pluviator was supported by four guide wheels and two electronically driven load wheels, which rest on the curb along the trench.

Sand was placed in the hopper using a backhoe. An electric motor was used to drive the pluviator along the length of the trench that also simultaneously rotated the distribution drum to spread the sand in a controlled, uniform manner. Field calibrations were conducted to control and accurately predict the in-situ unit weight during pluviation. Prior to sand placement, a staircase was developed along the bottom of the trench. Placed on each step were two containers, of known dimensions, for sand collection. The height from the dispensing tray of the pluviator to each container was known. The pluviator was then filled with sand and driven continuously over the containers until full. Any excess sand was carefully removed and the weight of each container was measured. Given the weight and known dimensions of each container, the approximate unit weight was determined. The calibration was performed six times with varied fall heights (38 mm to 830 mm), opening size to control sand flow (3 mm to 19 mm), and dispensing tray angle (40^o to 55^o). It was concluded that selecting the right combination of fall height, sand rate, and the angle of the dispensing tray could control the unit weight during pluviation. However, variability should be recognized.

Minicone penetrometer tests (MCPT) pushed between the anchors indicated some variability within the three test trenches. The unit weights for each anchor test were adjusted and determined from a site-specific CPT q_c-I_D (tip resistance-relative density) correlation. The unit weight with depth was back calculated at each MCPT location using the maximum and minimum unit weights for Golden Flint sand (Table 2). A median unit weight was then taken at each MCPT location from the surface to a corresponding anchor depth. Lastly, by corresponding the median MCPT unit weights on either side of an anchor test, a second median was taken to determine the unit

weight at the exact anchor location. Friction and dilatancy angles were then calculated from Equation 9 for each test (Table 4).

Anchor Test Results

Anchors were pulled out using a hydraulically powered load frame as shown in Figure 10. The loading frame had a 9 metric ton capacity and was equipped with four wheels at the base of the frame. Pullout tests were applied at a constant rate to fully develop the load-displacement behavior. The helical anchors were screwed into the test trench at variable rates and lowered using a winch and pulley system that was secured to the exterior of the frame. Displacements during installation and pullout were recorded using string potentiometers secured to the test frame. Lastly, a system of dead weights, as previously described, was used to provide downward force during installation. Installation occurred by a means of rotation into the soil by matching the vertical penetration rate with the RPMs to minimize soil disturbance.

Although soil disturbance may still seem apparent and affect the overall breakout capacity, tests were performed at varied installation rates and showed no change in capacity when compared to the other tests; Figure 11 displays the breakout capacity against the varied installation rates. Anchor pullout tests were performed at a constant rate using a linear actuator and winch system mount to the frame. A typical load versus displacement curve for a 254 mm diameter anchor at an embedment of 762 mm is shown in Figure 12. Table 4 summaries the results of each helical anchor pullout test.

EVALUATION OF THEORETICAL MODELS

Vertical pullout tests on large-scale, shallow, single-helix anchors have been performed and are used in this thesis to evaluate a range of theoretical breakout capacity models; the models have been collated and presented as an equivalent breakout factor, N_γ as shown in Table 1. Each model was evaluated using the soil properties (i.e. ϕ'_{peak} and ψ) established for each helical anchor test and then compared to the measured N_γ values. Comparisons are made against the limit equilibrium models, followed by the limit analysis and more sophisticated approaches (i.e. cavity expansion and finite element analyses). Assuming the data follows a lognormal distribution, the geometric average bias (predicted/measured) and standard deviation for all limit equilibrium, finite element, and cavity expansion models was calculated and shown in Table 5.

Limit Equilibrium

The limit equilibrium approach has been used throughout the literature to estimate breakout capacity of shallow embedded anchors in sand. The models of interest include Meyerhof & Adams (1968), Murray & Geddes (1987), Saeedy (1987), Sarac (1989), Ghaly & Hanna (1994), and Hanna et al. (2007). By satisfying basic equilibrium and by making simplifying assumptions a priori, an estimate of capacity is determined. The approach typically assumes a failure surface inclined at an angle, θ, that the shear stresses along the failure plane are fully mobilized, and some estimate of the lateral earth pressures typically as a function of friction angle and embedment ratio (D/B). Figures 13 to 19 shows the results of breakout capacity factor (N_γ) versus D/B

plotted against the measured results. A visual representation of the deviation between the predicted and measured N_γ is shown in Figures 20 and 21. For these solutions, all values exceeding 1 over-predict capacity while below 1 indicate an under-prediction.

The solutions presented by Meyerhof & Adams (1968) (Figure 13) and Murray & Geddes (1987) (Figure 14) show an over-prediction of anchor capacity. Both models over-predict capacity more at low relative density than at high relative density. From low to high relative density, the bias (predicted/measured) for Meyerhof & Adams ranges from 1.76 to 1.97 and 1.74 to 1.46 for Murray & Geddes. Both models produce similar estimates in breakout capacity but are based on different underlying assumptions. The model derived by Meyerhof & Adams assumes a smaller soil wedge relative to that of Murray & Geddes, thus less soil to be displaced during pullout. However, an earth pressure coefficient (K_u) ranging from 1 to 2 is used to develop their model, which leads to larger lateral earth pressures acting along the failure surface than K_o conditions assumed by Murray & Geddes. Uncertainty is evident among the development of the models presented by Meyerhof & Adams (1968) and Murray & Geddes (1987), however both provide similar predictions in breakout capacity; the results suggest there may be a compensating effect in the assumptions of the failure surface and lateral earth pressures.

Similarly, the solutions presented by Ghaly & Hanna (1994) (Figure 17) and Hanna et al. (2007) (Figure 18) over-predict breakout capacity considerably. On average, the breakout capacity predicted by both models is approximately 3 times larger than the measured at low relative density and 2.25 times larger at high relative density. The

failure surface assumed in the models is inclined at the plate edge at an angle of $45-\frac{\phi'}{2}$ which is similar to that used by Sarac (1989). The inclination of the failure surface contributes significantly to the breakout capacity; the greater the angle the larger the soil wedge, thus potentially increasing the capacity. In addition to, a form of passive pressures is suggested by both authors where K_p is greater than 2.5. Thus, the over estimate in capacity could be attributed to the larger failure wedge and larger lateral stresses. Also, the predicted breakout capacity was larger than both Saeedy (1987) (Figure 15) and Sarac (1989) (Figure 16) that assumed a similar failure surface and inclination angle.

Although the models presented by Saeedy (1987) and Sarac (1989) are similar to Ghaly & Hanna (1994) and Hanna et al. (2007) in the assumed failure surface, the estimate of lateral earth pressures is very different. Sarac uses a more complex method to describe the lateral earth pressures discussed in Berezancev (1952), while Saeedy sets the lateral earth pressure coefficient equal to 1. This subtle difference in lateral earth pressure defined by Saeedy (1987) and Sarac (1989) provides an estimate in capacity, on average, 1.50 times larger than the measured capacity. The predictions of the two models are also 1.50 times smaller than the predictions of Ghaly & Hanna and Hanna et al.

In contrast to the abovementioned limit equilibrium models, the re-derived model adapted from White et al. (2008) (Figure 19) in this study shows to under estimate anchor breakout capacity. The model in this study under-predicted capacity, on average, 0.77 times the measured capacity and thus having the lowest capacity

predictions of the limit equilibrium models. Non-associated flow was used to develop the model which inclines the failure wedge at angle equal to the dilatancy angle, ψ. At shallow depths anchors are subject to low confining stresses, which will affect the constitutive behavior of the sand and may cause significant dilation even in loose sands. Experimental tests to study the soil deformation around uplift plate anchors in sand (i.e. Lui et al, 2012) suggests that θ is in fact approximately equal to ψ which perhaps better represents reality when used in an equilibrium model. Therefore, by considering the dilatancy angle as the inclination of the failure surface the soil wedge is smaller than the previous models and may better represent the actual failure shape and soil response. In addition, lateral earth pressures have been assumed for this model to initially be at the lowest state that can naturally exist (at-rest or K_o). The results suggest that by considering both parameters a relatively accurate but conservative prediction of breakout capacity can be calculated.

Two main assumptions that are common among the limit equilibrium models is shape of the failure surface and the lateral earth pressures. Either independently or properly combined, the breakout capacity could be closely estimated. The size and inclination of the failure surface will govern the amount of soil that has to be overcome during breakout; as the inclination angle increases the weight of the soil wedge will increase and decrease as the angle decreases. In addition to, an estimate of lateral earth pressure is needed to calculate the forces acting perpendicular to the failure surface, therefore both contributing to possible changes in breakout capacity. Lateral earth pressures are exceptionally difficult and highly uncertain. There are estimates in lateral earth pressure coefficients through empirical relationships that vary from K_o (at-rest), K_a

(active), K_p (passive), and K_u (uplift). These estimates are seen throughout the literature and used in the models, which supports the high variability amongst them.

Limit Analysis

While limit equilibrium has been used to provide an exact estimate of capacity, limit analysis methods have been used to develop a capacity envelope or bound solution. Figure 22 displays an upper bound solution by Murray & Geddes (1987). The solution over-predicts capacity which is consistent with the theory. By searching for a failure surface that obeys associated flow ($\theta = \phi' = \psi$) and a mechanism that will cause the soil mass to yield, the upper bound solution should in fact be greater than that of the measured. This is caused by the over estimate in the soil wedge or weight of soil that has to be displaced during breakout and assuming that the soil has reached failure.

In contrast to an upper bound, Merifield et al. (2006) (Figure 23) utilizes a lower bound limit analysis approach. The method is defined using the associated flow rule and although the soil is assumed to be in a state of equilibrium, it over-predicts the breakout capacity. The associated flow rule assumes the friction angle and dilatancy angle to be identical which over estimates the degree of dilation in the soil. By overestimating the soil dilation, the size of the soil wedge and ultimately the collapse load will be larger than measured values. Therefore, for a lower bound solution such that the soil is in equilibrium, the prediction may always be larger than the true collapse load. A non-associated flow model may be more suitable because the dilatancy of the soil can be defined at a value closer to reality and adjusted to yield predictions smaller than the true load.

Additional Methods

The results of the additional methods are shown in Figures 24 to 26 and the deviation between the predicted and measured N_γ in Figure 27. Vesic (1971) (Figure 24) predicts breakout capacity as a function of embedment ratio and friction angle using close-surface cavity expansion theory. At low relative density the bias is equal to 0.90, indicating an accurate prediction of the measured capacity while at high density the bias lowers to 0.70. Similarly, both Rowe & Davis (1982) (Figure 25) and Sakai & Tanaka (1998) (Figure 26) use finite element analyses to estimate breakout capacity that provide an under-prediction of breakout capacity. The under-prediction may be attributed to the more complex approach in defining the weight of the displaced soil and lateral earth pressures, which is not done in most of the limit equilibrium models.

CONCLUSIONS

An accurate or conservative prediction of anchor breakout capacity in sand is a critical aspect in the safety of structures subjected to uplift loading both on and offshore. This thesis presents an evaluation of the theoretical capacity models compared against shallow embedded, large-scale, single-helix anchor experiments performed by the author. The database was developed by performing vertical pullout tests on helical anchors with diameters of 254 mm and 152 mm. Bolton's (1986) stress-dilatancy correlations were used to estimate the peak friction angles and dilatancy angles for each helical anchor pullout test and applied to the theoretical models. The following key conclusions can be drawn from the results presented in this thesis.

- More accurate predictions were obtained from non-associated flow limit equilibrium. The non-associated flow limit equilibrium in this study was the only model that under-predicted anchor breakout capacity relative to all the other limit equilibrium models presented. By defining the failure surface as $\theta = \psi$, the soil wedge is smaller relative to the other models; similarly, when at-rest pressure conditions are used the lateral stresses along that failure surface are smaller than the other models. Both parameters affect anchor breakout capacity, therefore results suggest that the lower they are the more accurately and conservative the prediction. The model re-derived in this study resulted with an average ratio of predicted to measured breakout capacity of 0.77.

- The upper bound limit analysis model by Murray & Geddes (1987) are consistent with the theory by over-predicting anchor breakout capacity. However, the lower bound model by Merifield et al. (2006) was inconsistent with a lower bound solution.

- The models by Vesic (1971), Rowe & Davis (1982), and Sakai & Tanaka (1998) utilize more sophisticated approaches to model soil behavior during breakout. Overall, the models primarily under-predicted capacity and showed an average predicted to measured breakout capacity of approximately 0.81, 0.38, and 1.22, respectively.

It is the author's opinion that accurate yet conservative predictive models should be considered for anchor breakout capacity. These models include; close-surface cavity

expansion presented by Vesic (1971), finite element analysis presented by Rowe & Davis (1982), limit analysis presented by Murray & Geddes (1987), and the non-associated flow limit equilibrium, re-derived in this study. However, the closed-form limit equilibrium solution re-derived in this study has one of the highest levels of accuracy and the lowest variability relative to the other models presented (ratio of predicted to measured breakout capacity of 0.77, σ_{ln} of 0.14) and provides a convenient closed form equation to estimate capacity.

Table 1: Theoretical models for shallow circular and helical anchors in literature.

Author Method	Analytical Method	Anchor Type	Equivalent Nγ Equation
Meyerhof & Adams (1968)	Limit Equilibrium	Cir. Plate	$N_\gamma = 2sk_u\frac{D}{B}\tan\phi' + 1 + 2\frac{D}{B}\tan\frac{\phi'}{3} + \left(\frac{D}{B}\right)^2\tan^2\frac{\phi'}{3} + \frac{W_{anchor}}{\frac{\pi}{4}\gamma' B^2 D}$
Murray & Geddes (1987)	Limit Equilibrium	Cir. Plate	$N_\gamma = 1 + 2\frac{D}{B}\left(\sin\phi' + \frac{\phi'}{2}\right)\left(1 + \frac{2}{3}\frac{D}{B}\tan\frac{\phi'}{2}\left(2 - \sin\phi'\right)\right)$
Saeedy (1987)	Limit Equilibrium	Cir. Plate	$N_\gamma = \frac{4}{\pi}F_{\gamma\phi}$ $F_{\gamma\phi}$ = see literature (Figure 2)
Sarac (1989)	Limit Equilibrium	Cir. Plate	See literature (Figure 2)
Ghaly & Hanna (1994)	Limit Equilibrium	Helical	$N_\gamma \frac{4}{\pi}\left(\frac{D}{B}\right)^2\left(FW_{ss} + FF_{ss}\right)$ FW_{ss} = See literature (Figure 2), FF_{ss} = See literature (Figure 4)
Hanna et al. (2007)	Limit Equilibrium	Helical	See literature (Figure7a)
Murray & Geddes (1987)	Limit Analysis	Cir. Plate	$1 \le N_\gamma \le 1 + 2\frac{D}{B}\tan\phi'\left(1 + \frac{2}{3}\frac{D}{B}\tan\phi'\right)$
Merifield et al. (2006)	Limit Analysis	Cir. Plate	See literature (Figure 7)
Vesic (1971)	Close-Surface Cavity Expansion	Cir. Plate	See literature (Table 2)
Rowe & Davis (1982)	Elasto-Plastic Finite Element Analysis	General	$N_\gamma = F_\gamma R_\psi R_R R_K$ $R_\psi = 1 + \left(\frac{\psi}{\phi}\right)\left(R_{\psi=\phi} - R_o\right)$ F_γ = See literature (Figure 5), R_R = 1 (smooth surface), R_K = 1
Sakai & Tanaka (1998)	Finite Element Analysis	Cir. Plate	See literature (Figure 9)

Nγ = anchor breakout factor, D = embedment depth, B = anchor diameter, ϕ' = peak friction angle, ψ = dilatancy angle, γ' = buoyant unit weight

Table 2: Measured Properties of Test Soil.

Property	Value
γ_{max} (kN/m^3)	17.68
γ_{min} (kN/m^3)	14.24
e_{max}	0.847
e_{min}	0.487
G_s	2.68
D_{50} (mm)	0.250
C_u	1.61
C_C	1.13

Table 3: Consolidated Drained Triaxial Test Results.

Sample	σ'_3	σ'_1	p'_p	I_D	ϕ'_{peak}
	kPa	kPa	kPa		deg
1*	34.5	147	71.8	0.190	38.3
2*	34.5	165	78.1	0.350	40.9
3*	34.5	188	85.7	0.520	43.7
4*	34.5	206	91.7	0.640	45.5
5*	34.5	221	96.6	0.730	46.9
6*	34.5	228	98.8	0.770	47.5
7**	30.0	113	57.8	0.048	37.5
8**	30.0	178	79.5	0.396	45.4
9**	30.0	193	84.3	0.600	46.9

* Results obtained from Tufenkjian & Yee (2006) on Golden Flint sand

**Results obtained from this study on Golden Flint sand

Table 4: Summary of helical anchor test results.

Test ID	γ'	ϕ'_{peak}	ψ	Diameter B	Depth D	D/B	Rotation Rate	Installation Rate	Peak Breakout Capacity Q_u	Disp. At Peak Breakout Capacity
	kN/m^3	deg	deg	mm	mm		RPM	mm/s	N	mm
1-a*	14.89	41.8	12.2	254	785	3.1	41	20	4003	33
1-b*	14.73	40.6	10.8	254	787	3.1	44	18	3748	33
1-c*	14.78	41.0	11.3	254	762	3.0	44	22	3685	33
1-d*	14.80	41.1	11.4	254	762	3.0	44	29	3869	33
1-e**	14.94	42.2	12.8	254	730	2.9	42	34	4320	20
1-f**	15.02	42.8	13.5	254	727	2.9	42	38	5355	14
1-g**	14.85	41.5	11.9	254	733	2.9	42	33	5374	19
1-h**	14.74	40.7	10.8	254	794	3.1	42	39	3824	39
1-i*	14.71	40.4	10.5	254	775	3.1	43	20	3897	33
1-j*	14.70	40.4	10.5	254	775	3.1	44	23	3814	30
2-a*	15.72	47.7	19.6	254	737	2.9	40	26	6643	11
2-b*	15.77	48.1	20.1	254	721	2.8	41	26	6756	12
2-c*	15.77	48.0	20.0	254	775	3.1	41	29	7531	10
2-d**	15.61	46.9	18.6	254	787	3.1	19	15	7568	14
2-e**	15.62	47.0	18.8	254	756	3.0	16	10	6502	24
2-f*	15.63	47.1	18.9	152.4	762	5.0	43	26	4739	26
2-g*	15.64	47.1	18.9	152.4	756	5.0	42	25	4572	13
2-h*	15.47	46.6	18.3	254	460	1.8	43	36	1561	9
2-i*	15.56	47.3	19.2	152.4	448	2.9	43	26	1607	12
2-j*	15.16	44.4	15.5	152.4	435	2.9	43	26	1324	12
3-a*	15.47	45.6	17.0	152.4	1085	7.1	43	18	7335	17
3-b*	15.45	45.5	16.9	152.4	1031	6.8	43	18	7135	18
3-c*	15.43	45.5	16.8	152.4	938	6.2	43	31	5750	21
3-d*	15.44	45.8	17.3	152.4	756	5.0	43	19	4531	15
3-e*	15.37	45.3	16.6	254	775	3.1	33	16	5818	11
3-f*	15.34	45.1	16.4	254	762	3.0	25	16	5838	23
3-g*	15.31	44.8	16.0	254	806	3.2	32	7	5639	17
3-h*	15.25	44.4	15.6	254	781	3.1	24	17	5831	11
3-i*	15.27	44.8	16.3	254	488	1.9	25	17	2080	5
3-j*	15.29	45.3	16.7	152.4	438	2.9	43	21	1088	22

*Constant Rate

** Constant Force

Table 5: Statistical summary of calculated bias (predicted/measured) for limit equilibrium, cavity expansion, and finite element analyses.

Method	Geometric Mean	Log-Normal Standard Deviation σ_{ln}
Meyerhof & Adams (1968)	1.90	0.20
Murray & Geddes (1987)	1.62	0.20
Saeedy (1987)	1.46	0.19
Sarac (1989)	1.50	0.19
Ghaly & Hanna (1994)	2.36	0.19
Hanna et al. (2007)	2.57	0.17
This study	0.77	0.14
Vesic (1971)	0.81	0.21
Rowe & Davis (1982)	0.38	0.23
Sakai & Tanaka (1998)	1.22	0.23

Figure 1: Typical helical anchor configurations (adopted from Atlas Piers, 2014).

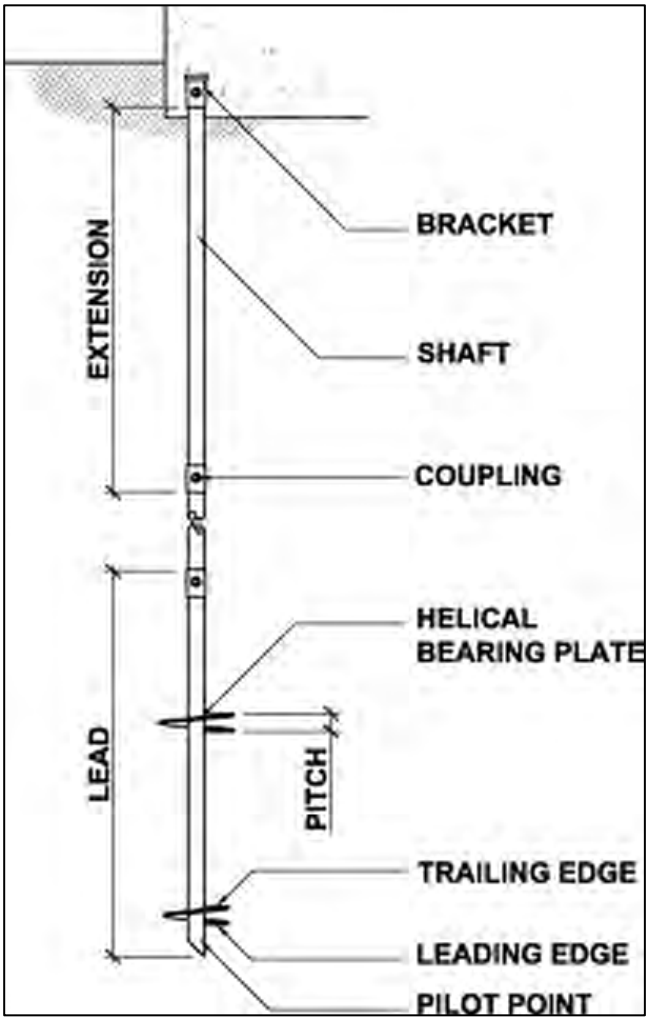

Figure 2: Typical multi-helix design (adopted from Perko, 2009).

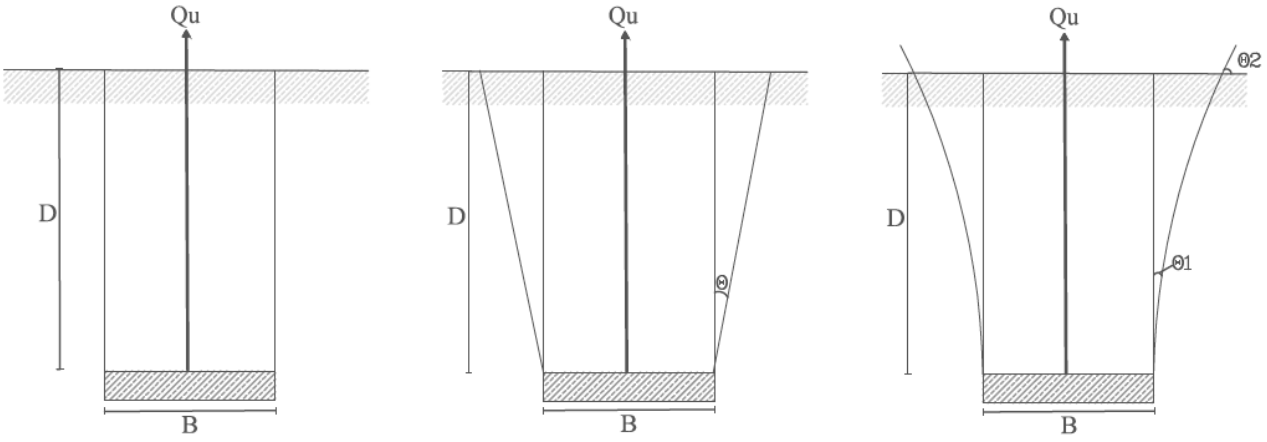

Figure 3: Three different failure modes for shallow embedded anchors in sand: (a) frictional cylinder; (b) truncated cone; (c) circular failure surface (adapted from Lui et al., 2012).

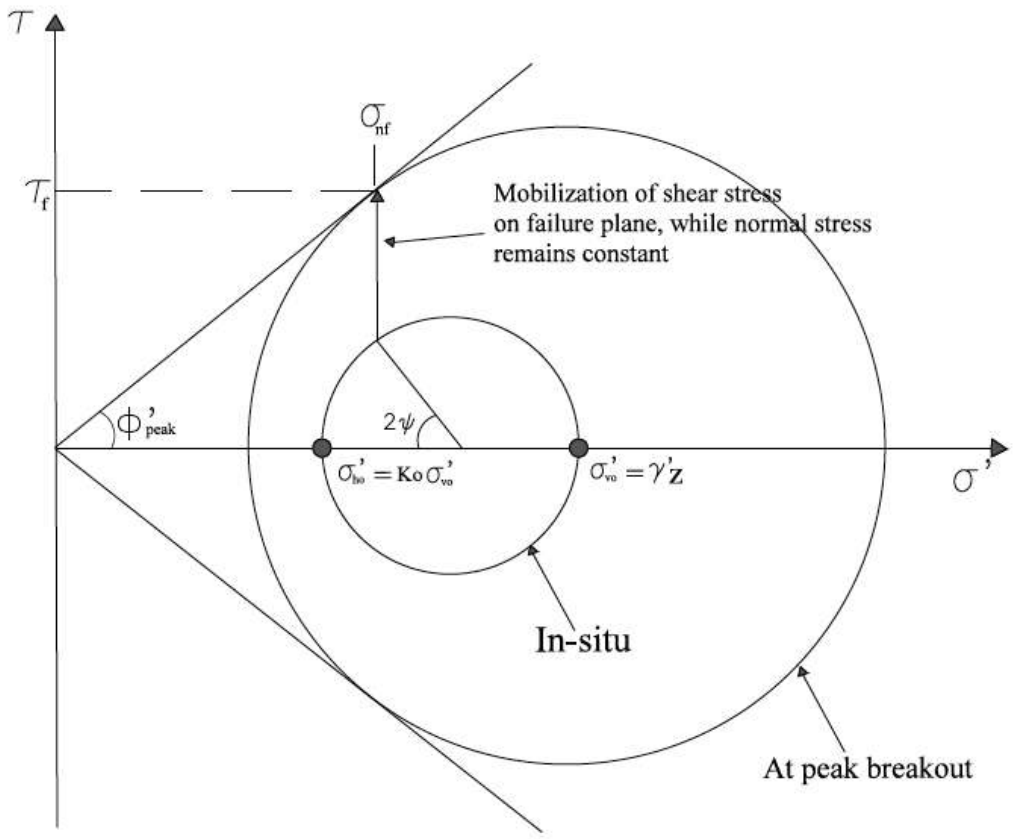

Figure 4: Assumed Mohr's circles in-situ and at peak breakout resistance for derivation of new limit equilibrium capacity model (adapted from White et al., 2008).

Figure 5: Test anchors (B = 152 mm, Total Length = 597 mm; B = 254 mm, Total Length = 616 mm).

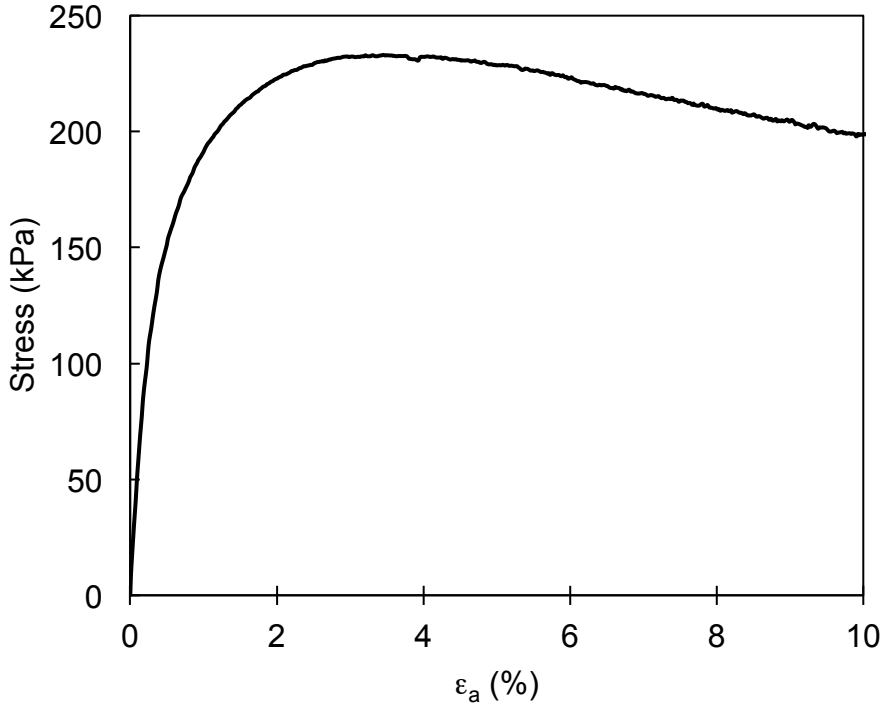

(a)

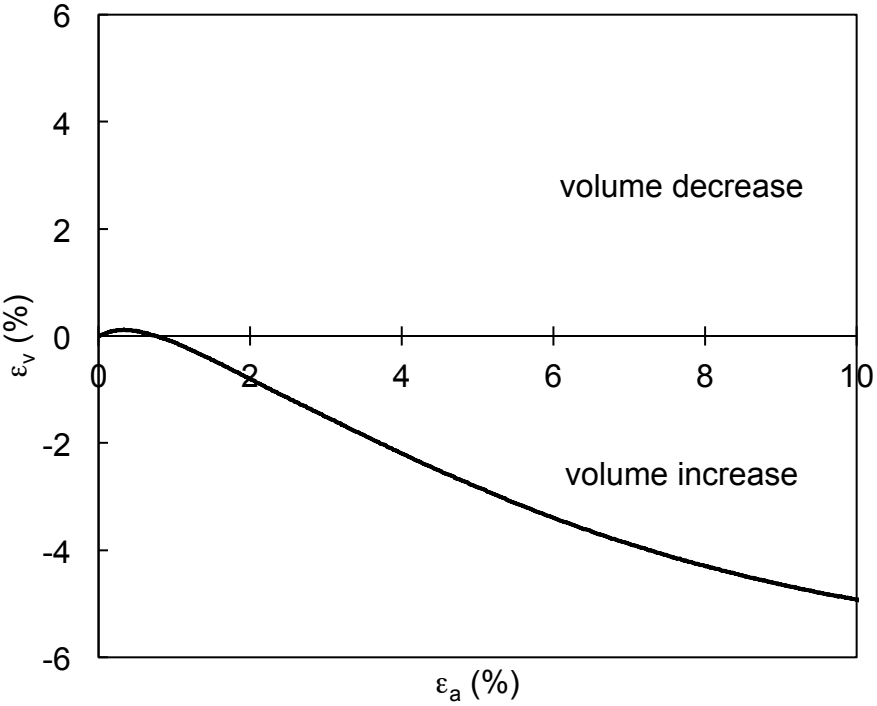

(b)

Figure 6: (a) Typical stress-strain of Golden Flint sand; (b) Typical volumetric strain vs. axial strain for Golden Flint sand.

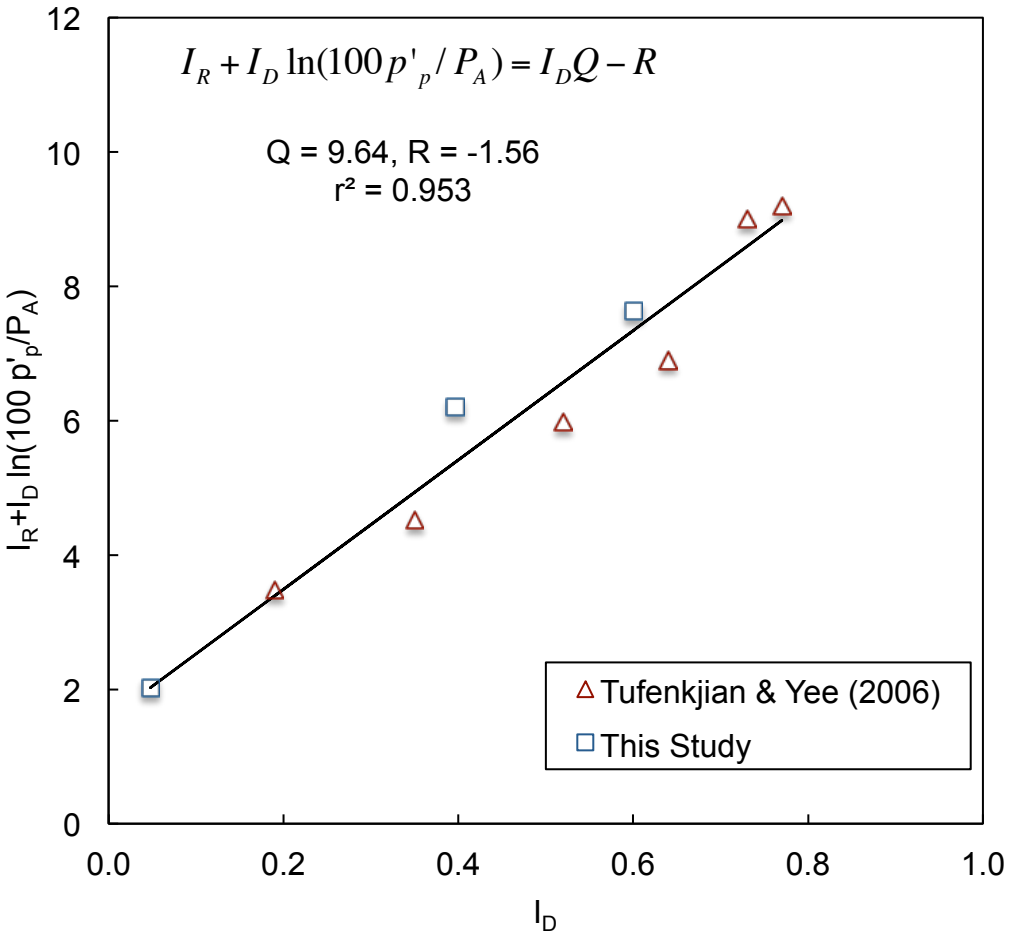

Figure 7: Visual illustration of best-fit Q and R-values for triaxial tests on Golden Flint Sand.

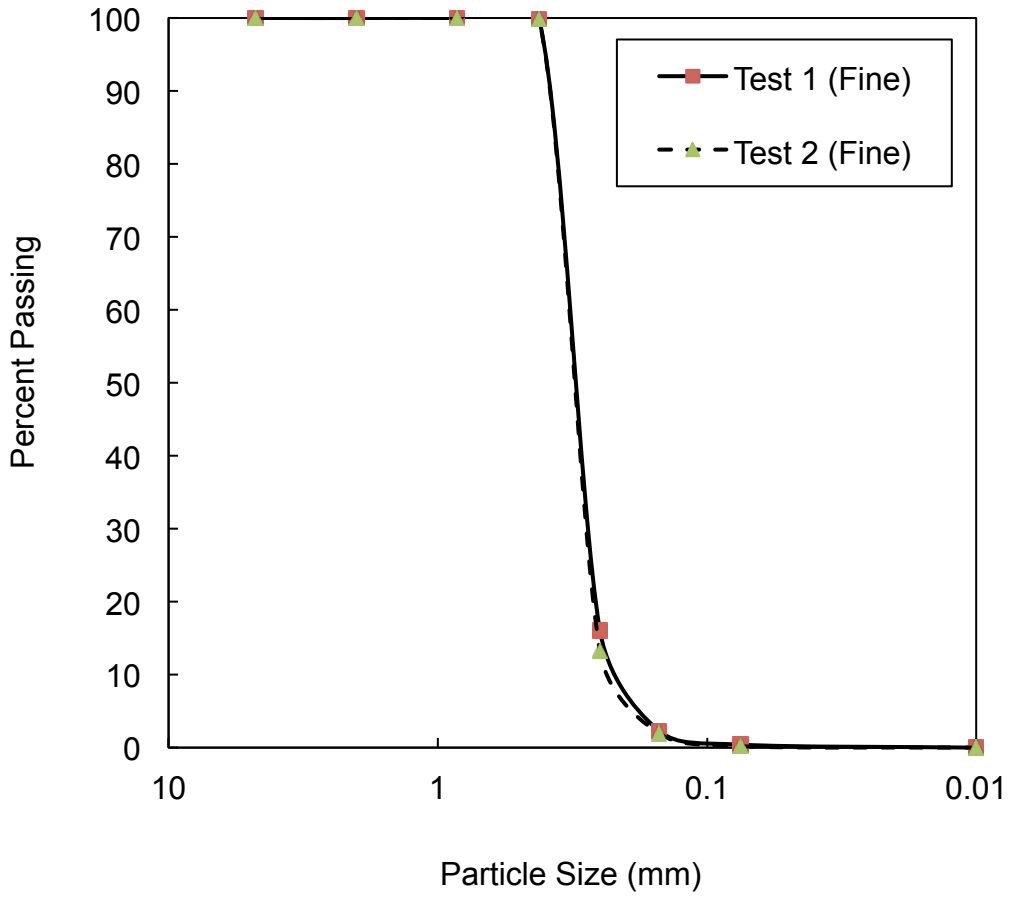

Figure 8: Gradation curve for Golden Flint Sand.

Figure 9: Sand pluviator used for test sample preparation.

Figure 10: Helical anchor load frame.

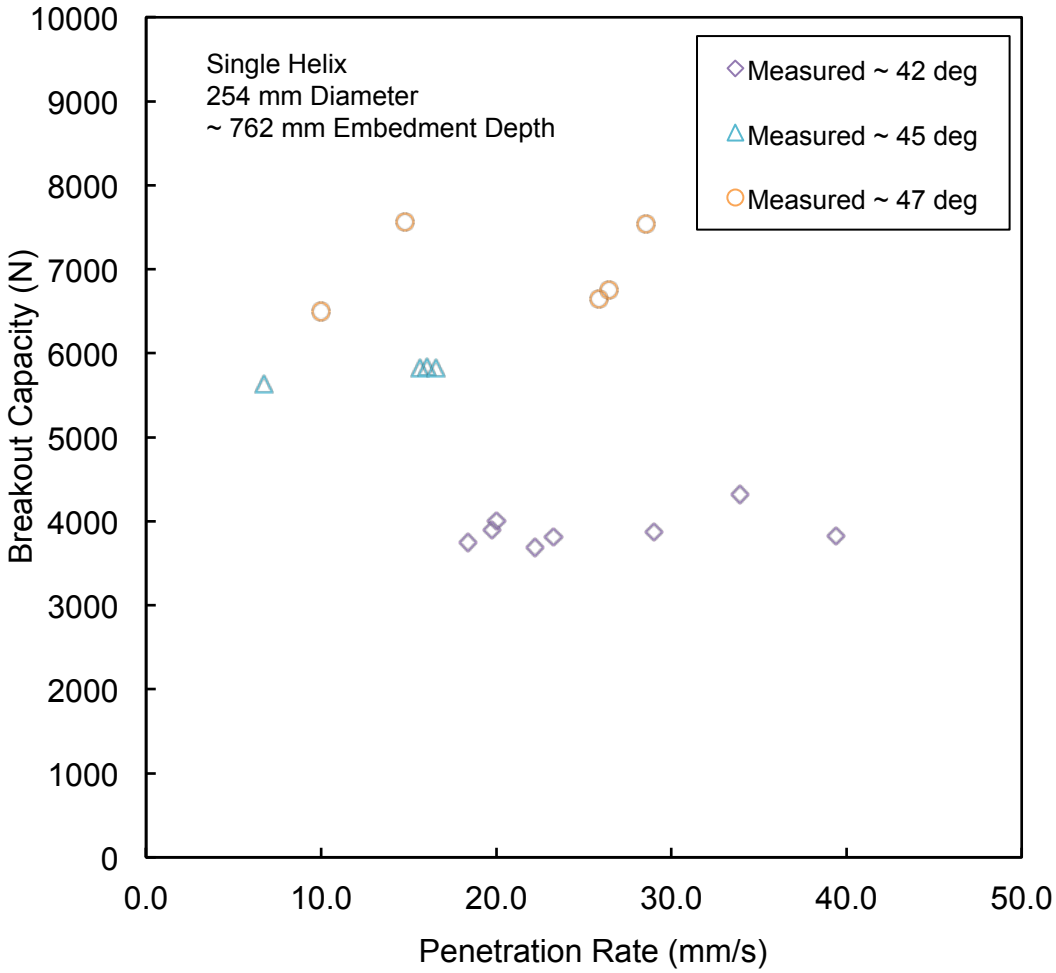

Figure 11: Measured breakout capacity vs. penetration rate for 254 mm diameter anchor at 762 mm embedment.

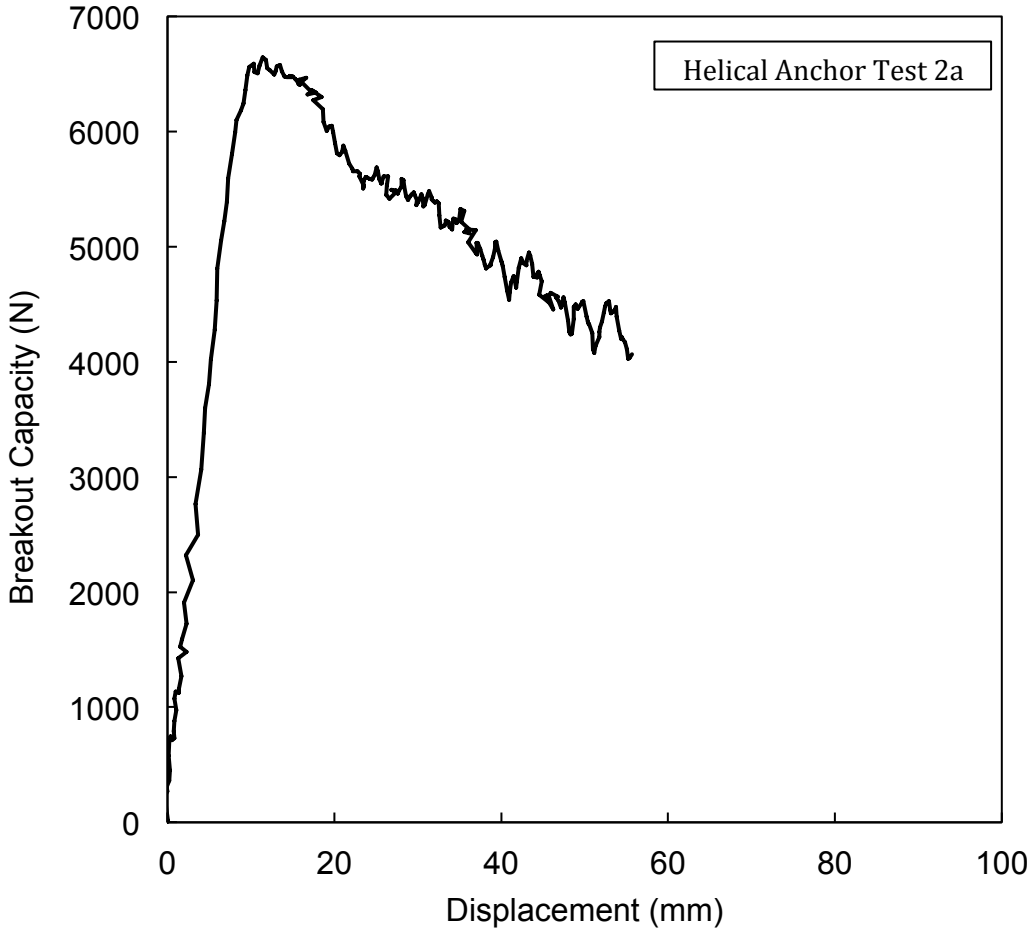

Figure 12: Typical measure load-displacement curve for a 254 mm diameter anchor at 737 mm embedment.

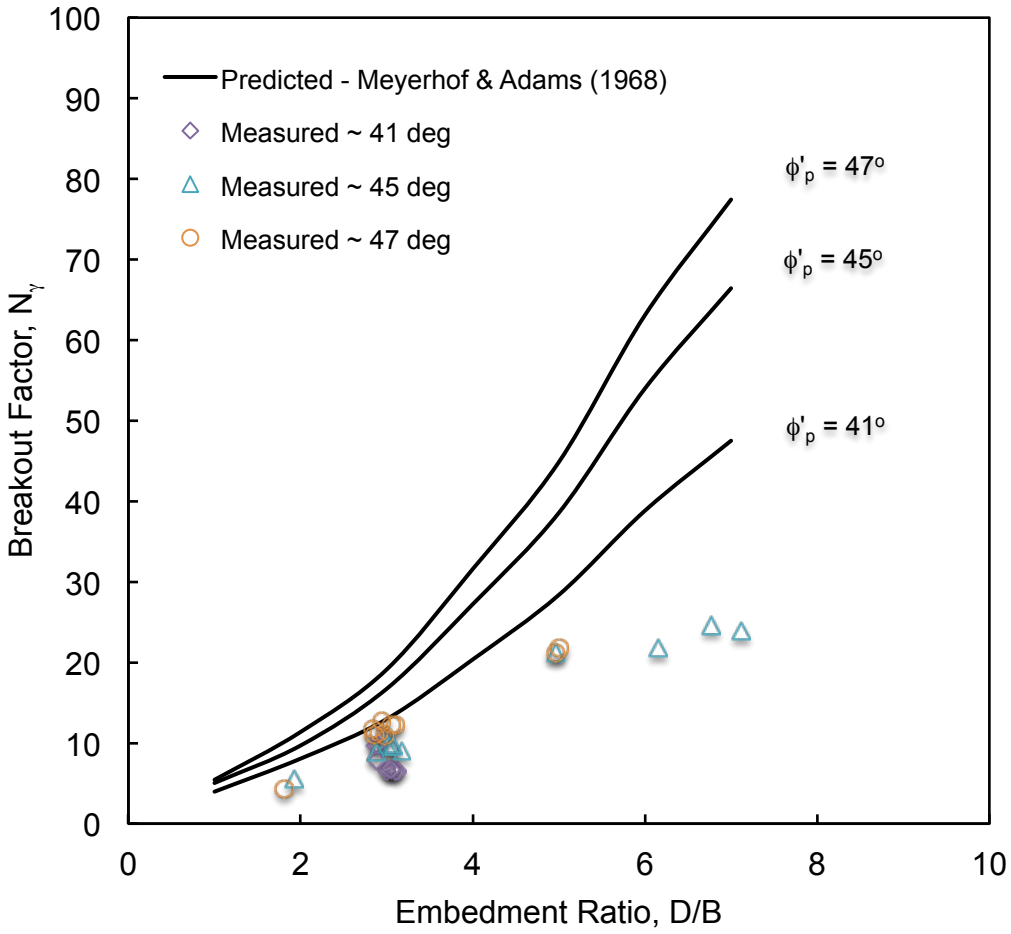

Figure 13: Nγ vs. D/B after limit equilibrium solution presented by Meyerhof & Adams (1968).

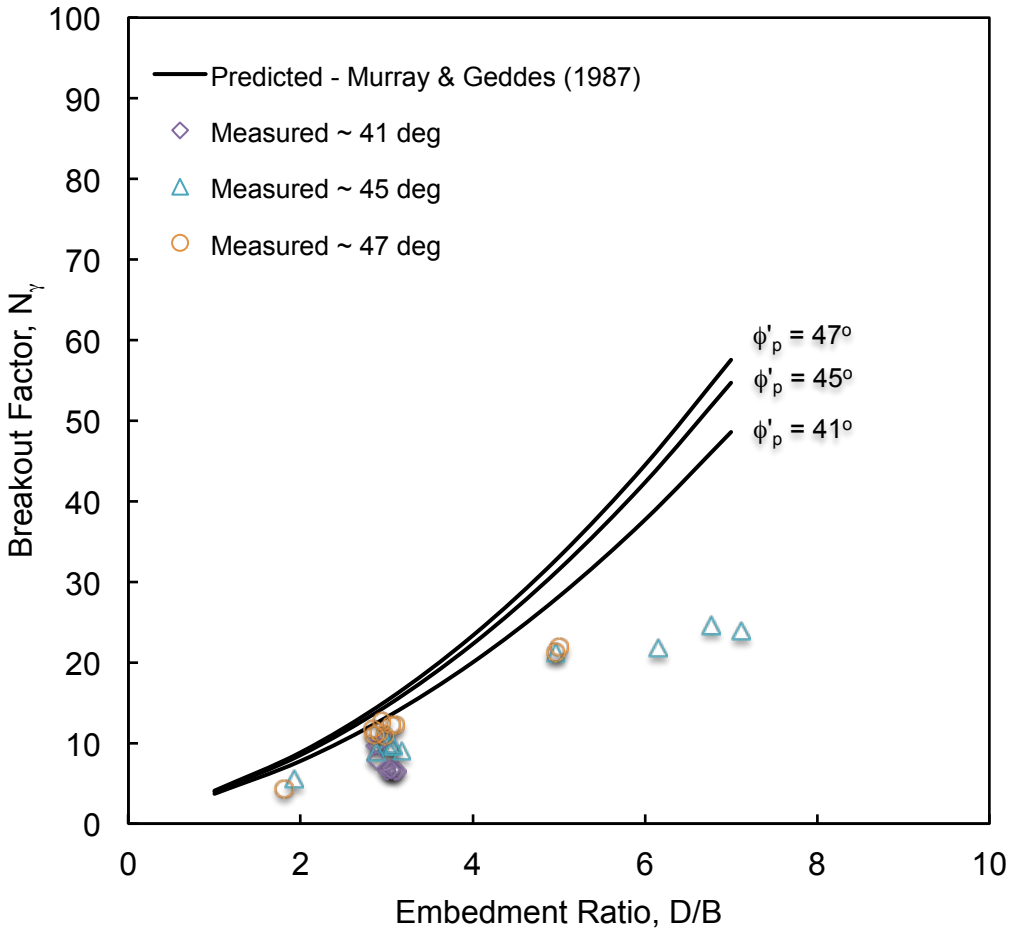

Figure 14: Nγ vs. D/B after limit equilibrium solution presented by Murray & Geddes (1987).

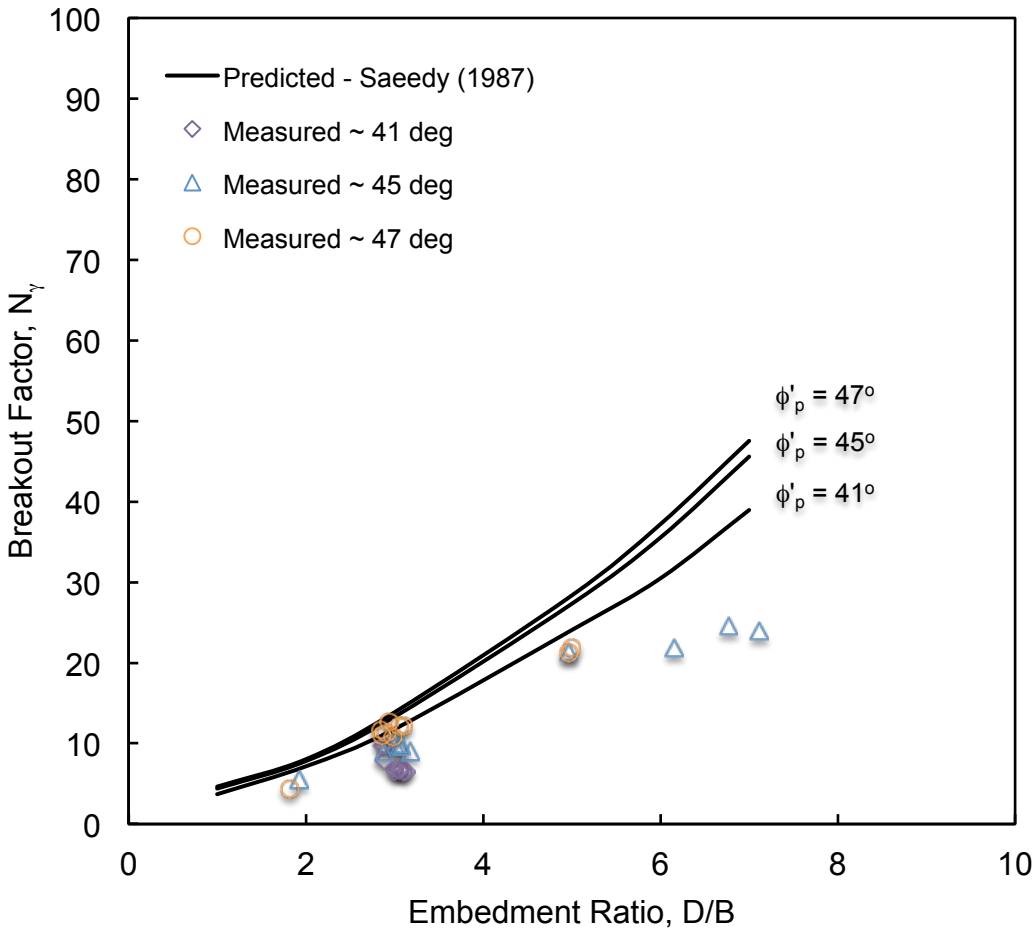

Figure 15: Nγ vs. D/B after limit equilibrium solution presented by Saeedy (1987).

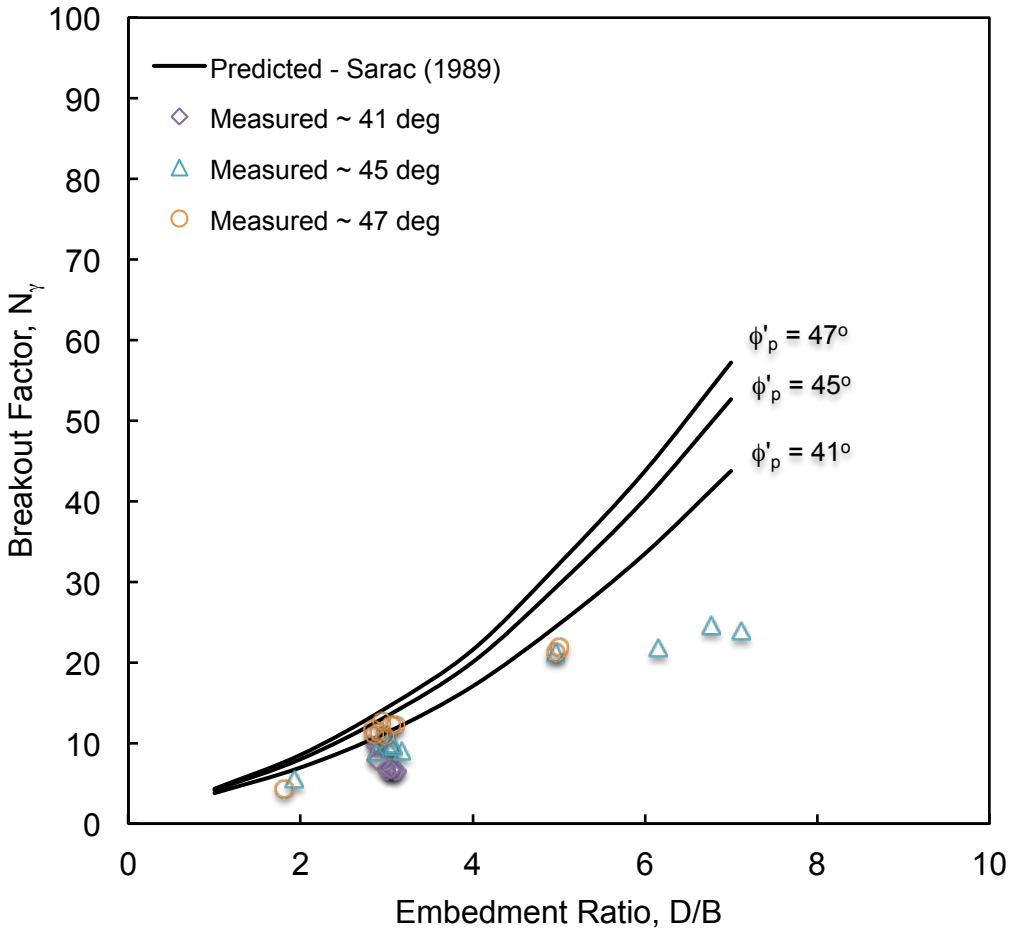

Figure 16: Nγ vs. D/B after limit equilibrium solution presented by Sarac (1989).

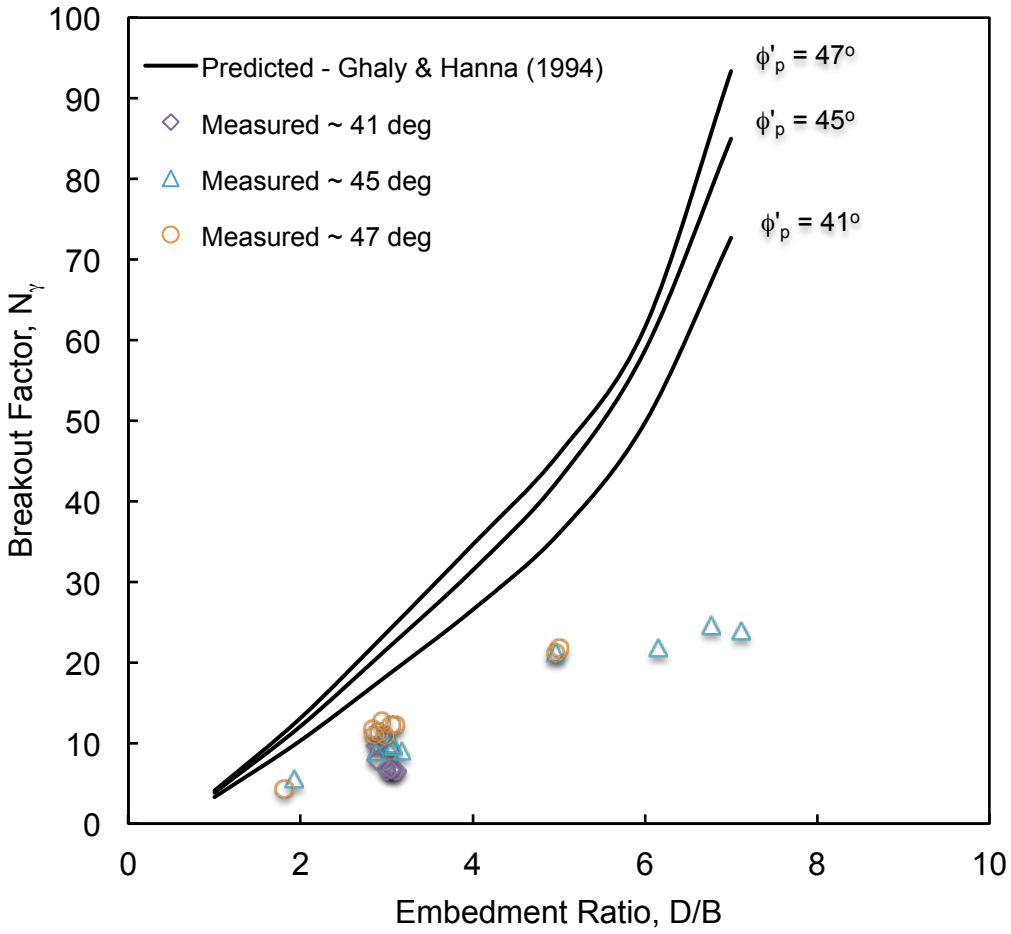

Figure 17: Nγ vs. D/B after limit equilibrium solution presented by Ghaly & Hanna (1994).

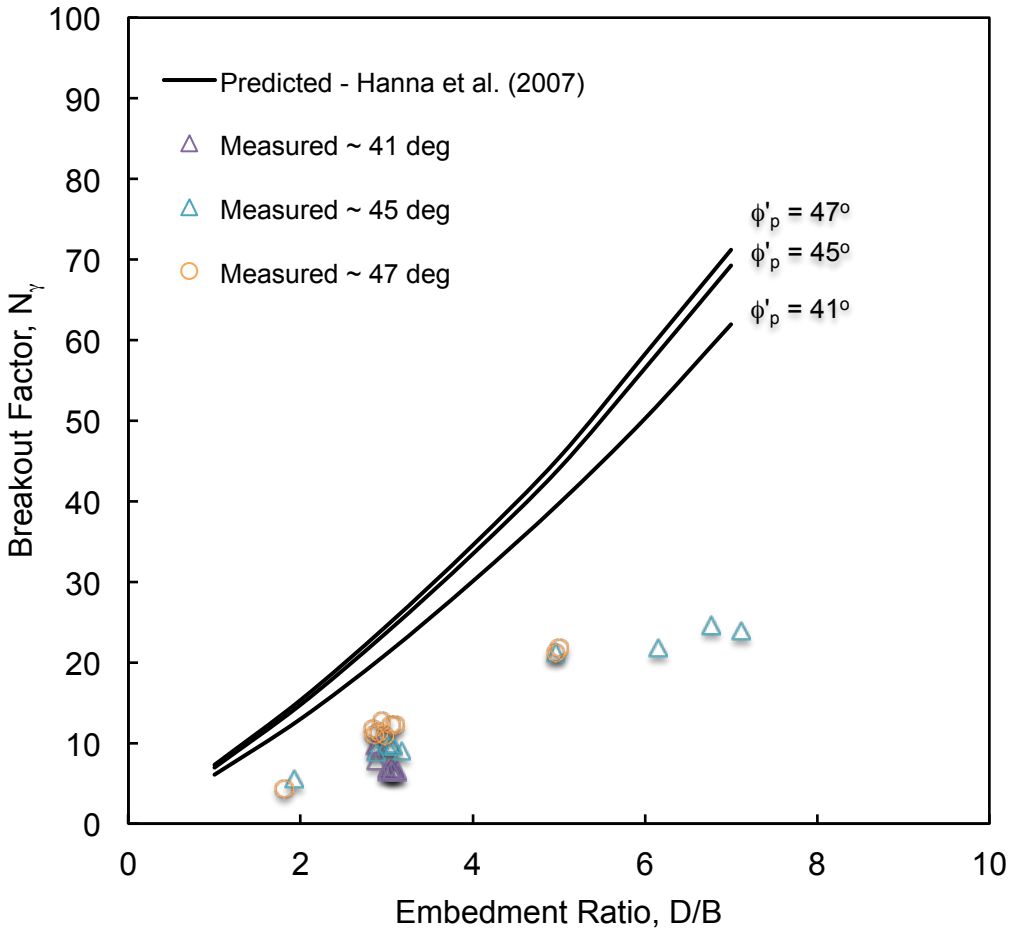

Figure 18: Nγ vs. D/B after limit equilibrium solution presented by Hanna et al. (2007).

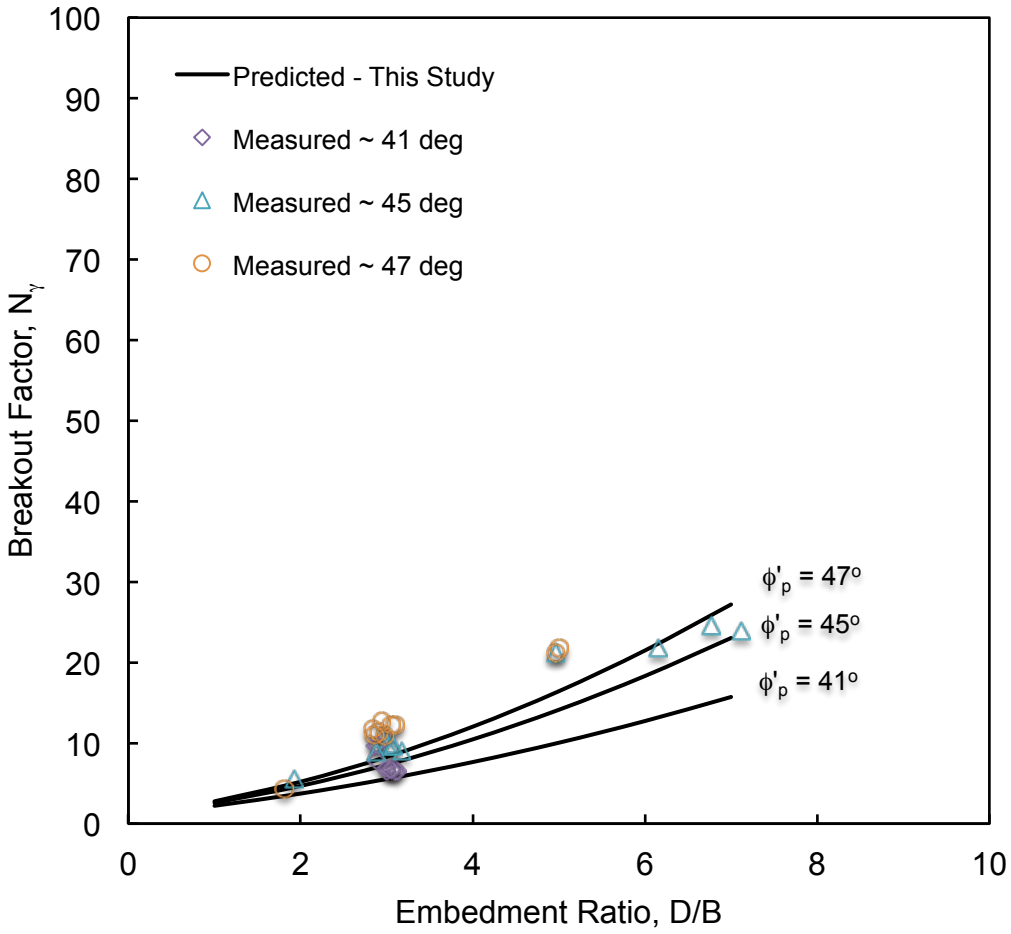

Figure 19: Nγ vs. D/B after limit equilibrium solution proposed in this study.

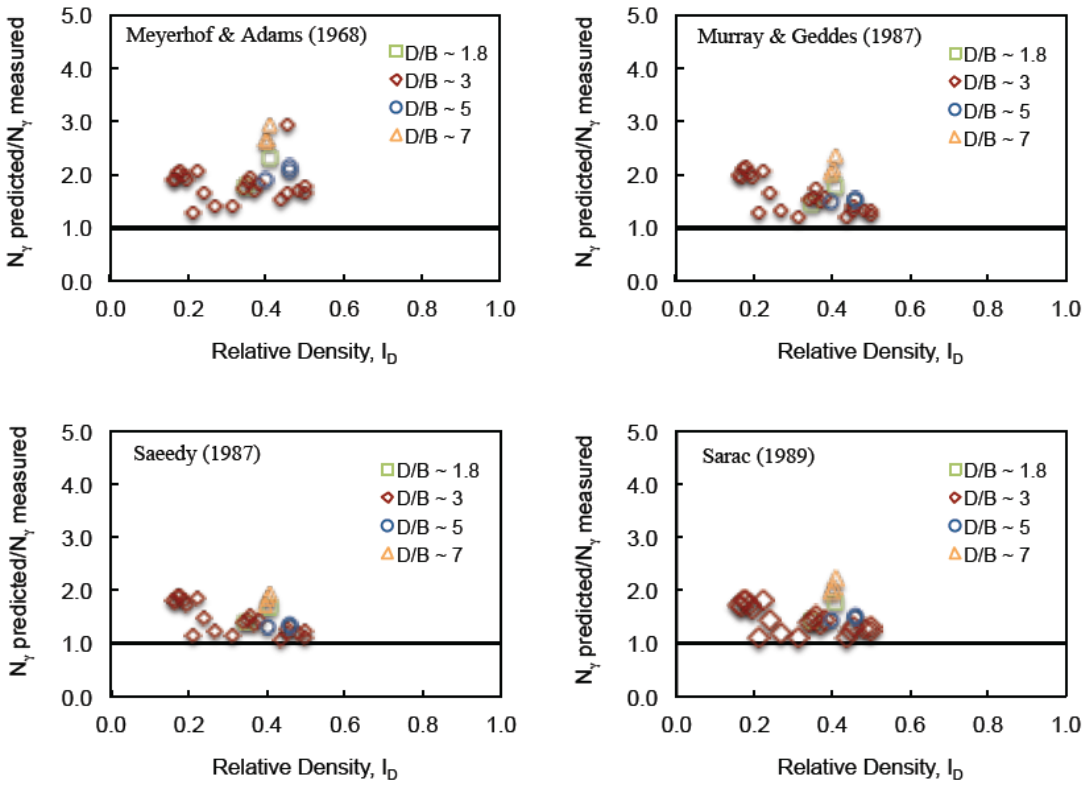

Figure 20: Ratio of Nγ (predicted/measured) vs. relative density for limit equilibrium solutions by Meyerhof & Adams (1968), Murray & Geddes (1987), Saeedy (1987), and Sarac (1989).

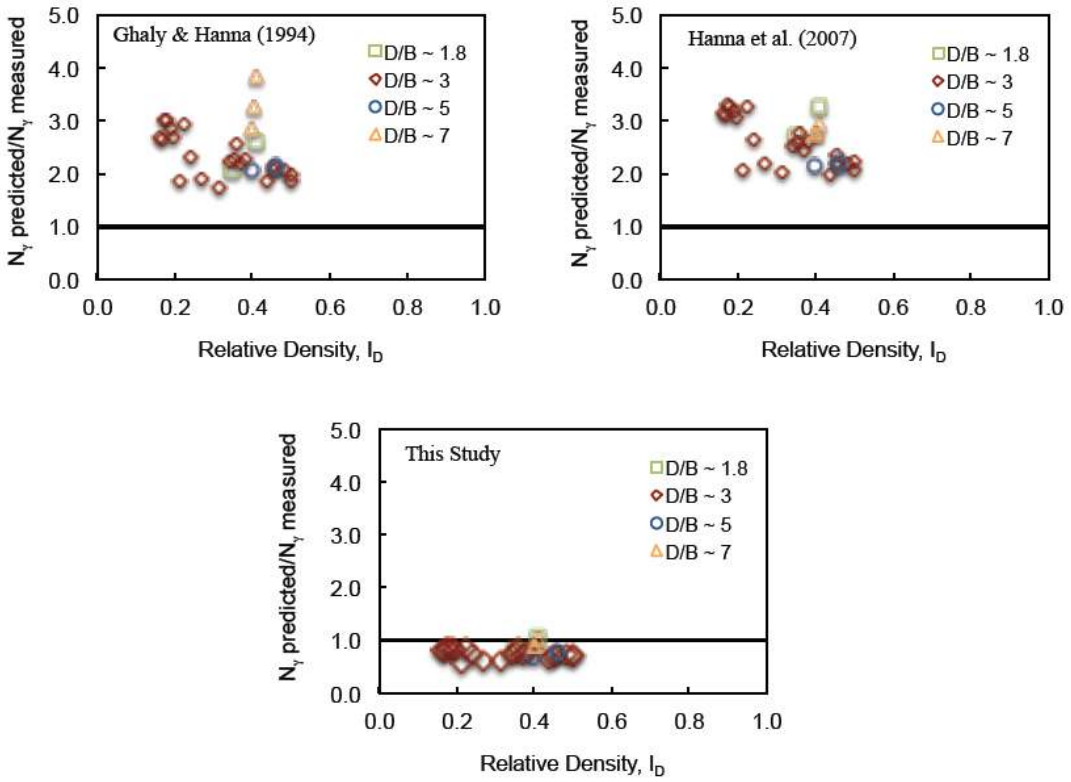

Figure 21: Ratio of Nγ (predicted/measured) vs. relative density for limit equilibrium solutions after Ghaly & Hanna (1994), Hanna et al. (2007), and this study.

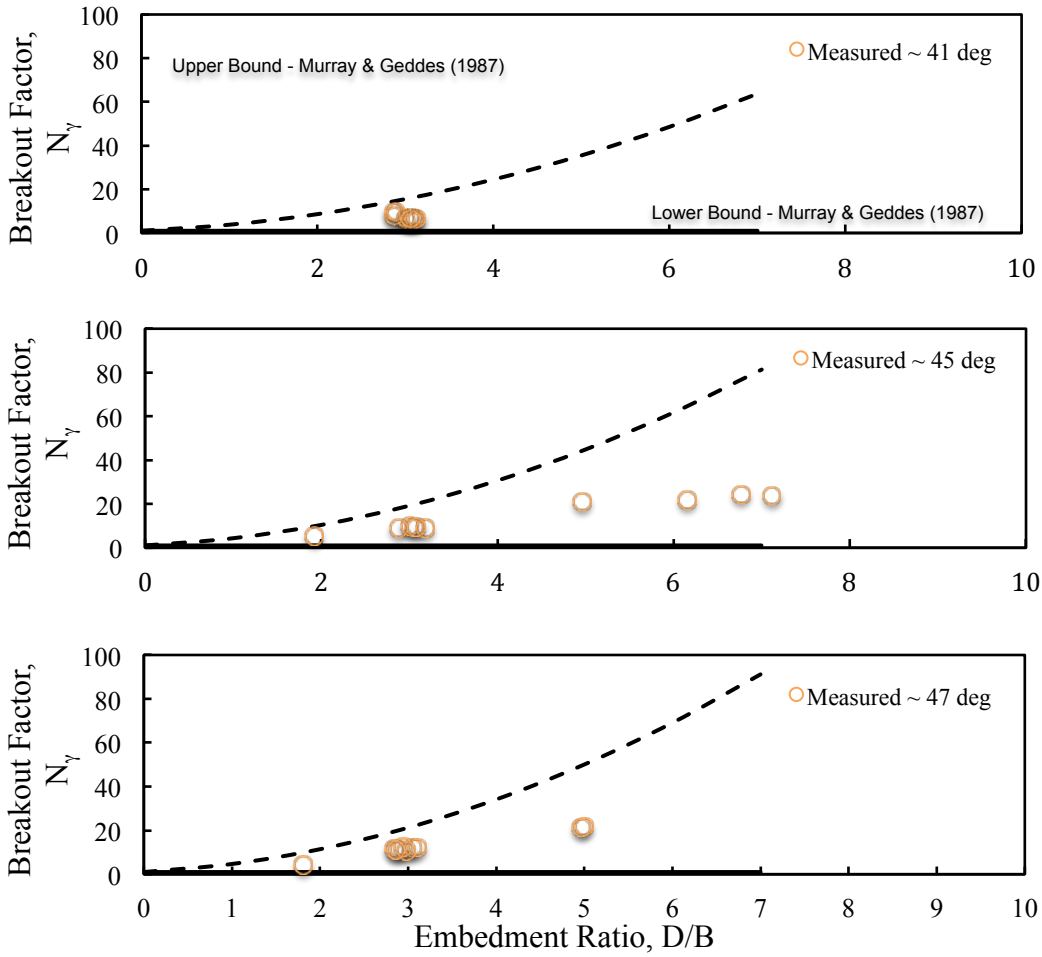

Figure 22: Nγ vs. D/B after limit analysis solution presented by Murray & Geddes (1987).

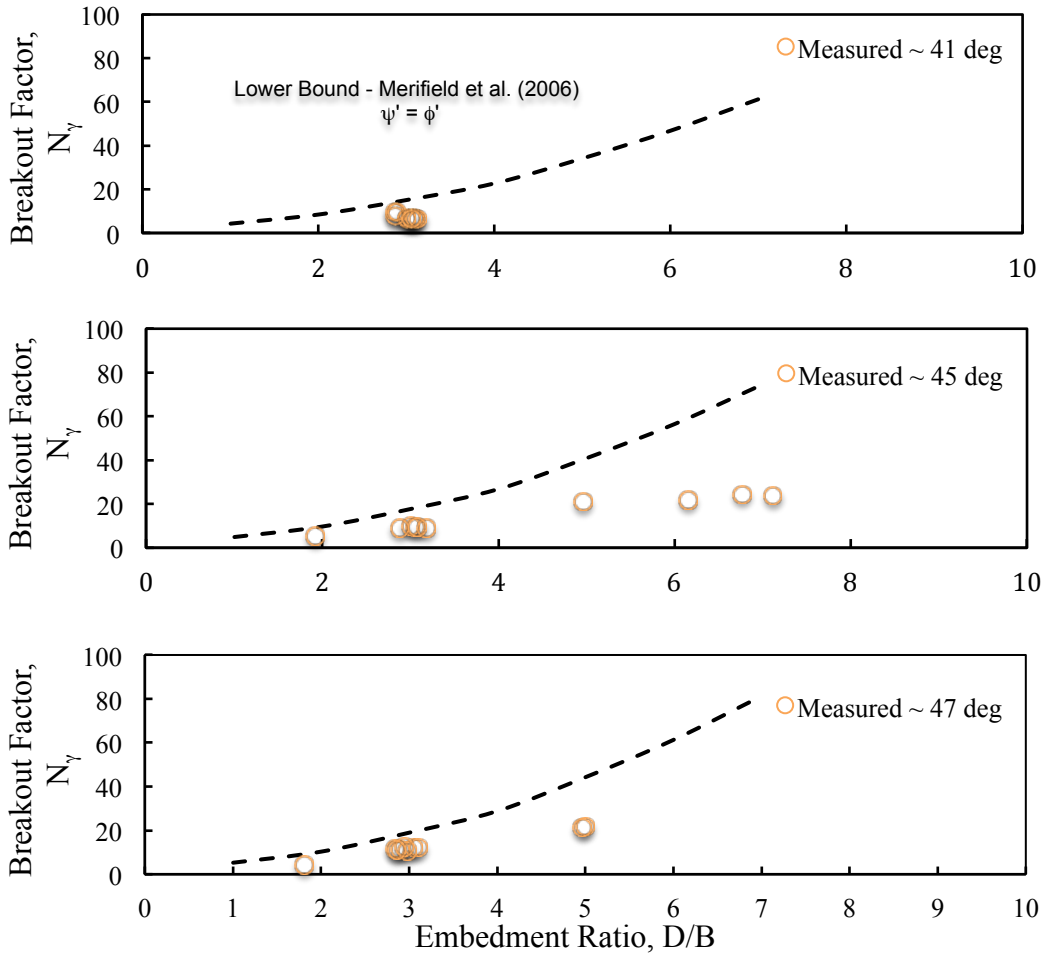

Figure 23: Nγ vs. D/B after limit analysis solution presented by Merifield et al. (2006).

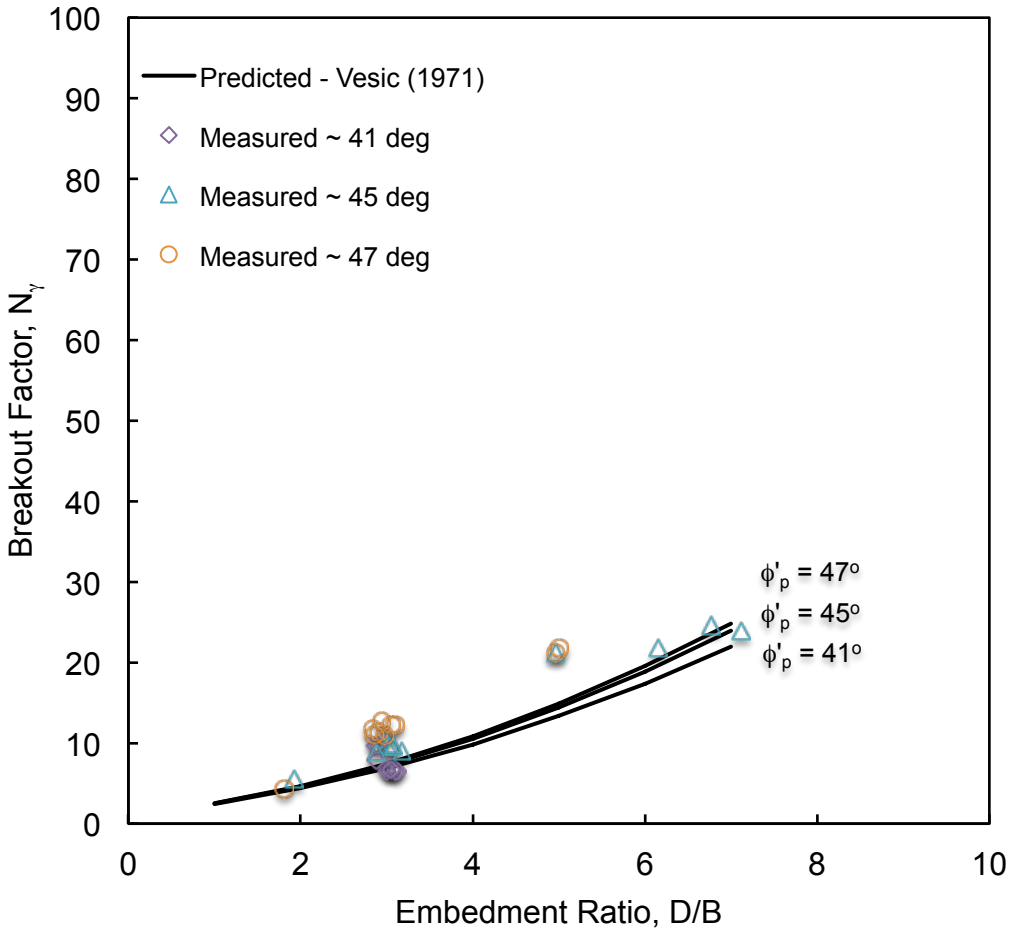

Figure 24: Nγ vs. D/B after close-surface cavity expansion solution presented by Vesic (1971).

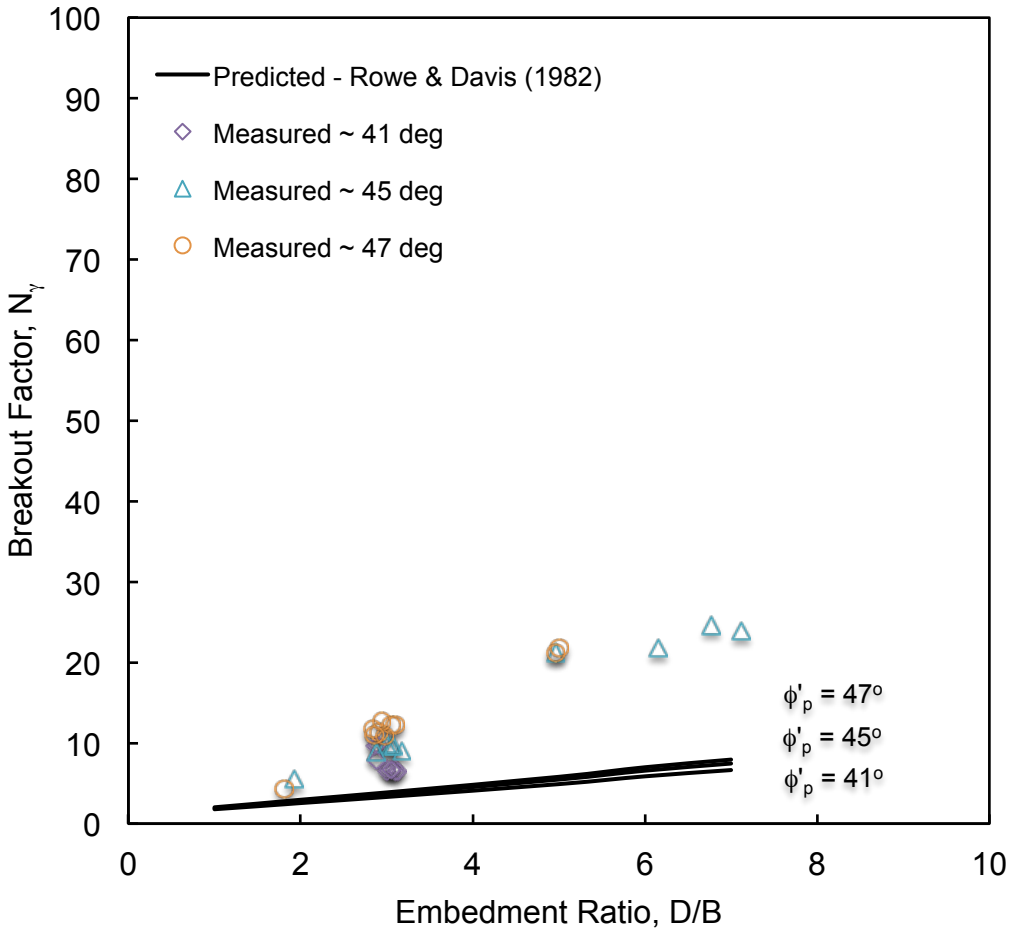

Figure 25: Nγ vs. D/B after elasto-plastic finite element analysis by Rowe & Davis (1982).

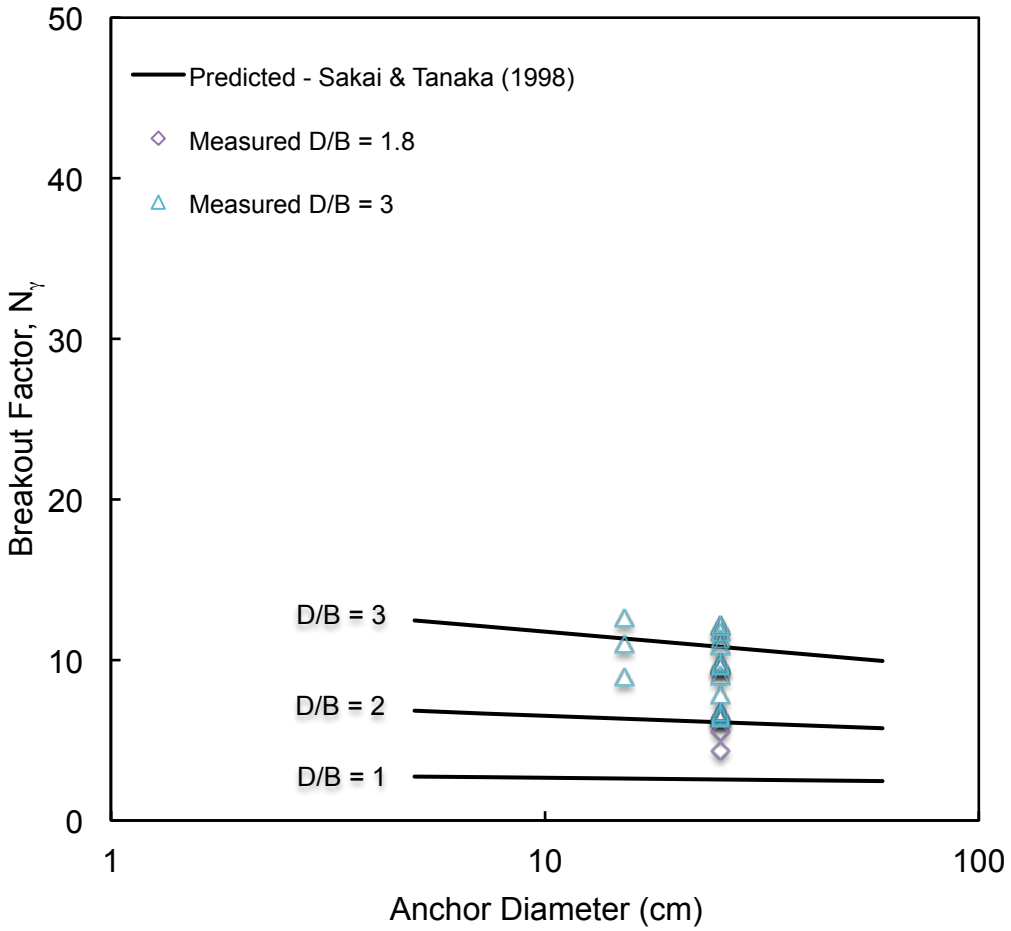

Figure 26: Nγ vs. anchor diameter after finite element analysis by Sakai & Tanaka (1998).

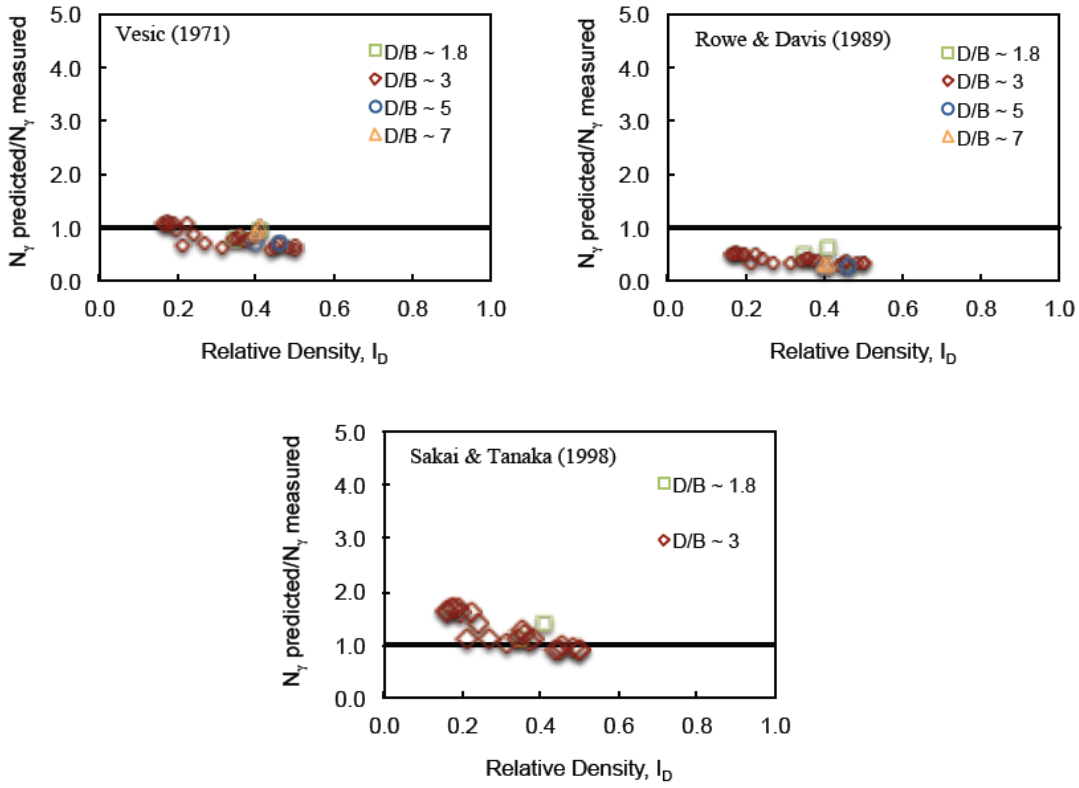

Figure 27: Ratio of Nγ (predicted/measured) vs. relative density after Vesic (1971), Rowe & Davis (1982), and Sakai & Tanaka (1998).

REFERENCES

Andreadis, A., Burley, E., & Harvey, R. (1981). Embedded anchor response to uplift loading. *Journal of the Geotechnical Engineering Division , 107* (1), 59-78.

Atlas Piers. (2014). *Merit Structures*. Retrieved Feburary 15, 2014, from Atlas Piers: http://www.meritstructures.com

Baker, W. H., & Konder, R. L. (1966). Pullout load capacity of circular earth anchor buried in sand. *44th Annual Meeting of the Highway Research Board. 108*, pp. 1-10. Washington District of Columbia: Highway Research Board.

Balla, A. (1961). The resistance of breaking-out mushroom foundations for pylons. *International Conference of Soil Mechanics and Foundation Engineering*, *1*, pp. 569-576. Paris.

Bolton, M. D. (1986). The strength and dilatency of sands. *Geotechnique , 36* (1), 65-78.

Chakraborty, T., & Salgado, R. (2010). Dilatancy and shear strength of sand at low confining pressures. *Journal of Geotechnical and Geoenvironmental Engineering , 136* (3), 527-532.

Chen, & Scawthorn. (1968). *Limit analysis and limit equilibrium solutions in soil mechanics.* Lehigh University, Civil and Environmental Engineering. Fritz Laboratory Reports.

Ghaly, A. M. (1995). Drivability and pullout resistance of helical units in saturated sands. *Soils and Foundations , 35* (2), 61-66.

Ghaly, A. M., & Clemence, S. P. (1998). Pullout performance of inclined helical screw anchors in sand. *Journal of Geotechnical and Geoenvironmental Engineering , 124* (7), 617-627.

Ghaly, A., & Hanna, A. (1994). Ultimate pullout resistance of single vertical anchors. *Candian Geotechnical Journal , 31*, 661-672.

Hanna, A., Ayadat, T., & Sabry, M. (2007). Pullout resistance of single vertical shallow helical and plate anchors in sand. *Geotech. Geol. Eng.* , 559-573.

Houlsby, G. T. (1991). How the dilatancy of soils affects their behaviour. *10th European Conference on Soil Mechanics and Foundation Engineering* (pp. 1-30). Italy: Universit of Oxford, Department of Engineering Science.

Ilamparuthi, K., Dickin, E. A., & Muthukrisnaiah, K. (2002). Experimental investigation of the uplift behavior of circular plate anchors embedded in sand. *Candian Geotechnical Journal , 39*, 648-664.

Lui, J., Liu, M., & Zhu, Z. (2012). Sand Deformation around an Uplift Plate Anchor. *Geotechnical and Geoenvironmental Engineering , 138* (6).

Lutenegger, A. J. (2011). Historical Development of Iron Screw-Pile Foundations: 1836-1900. *International Journal for the History of Engineering and Technology , 81* (1), 108-128.

Merifield, R. S., & Sloan, S. W. (2006). The ultimate pullout capacity of anchors in frictional soils. *Candian Geotechnical Journal , 43*, 852-868.

Merifield, R. S., Lymain, A. V., & Sloan, S. W. (2006). Three dimensional lower bound solutions for the stability of plate anchors in sand. *Geotechnique , 56* (2), 123-132.

Meyerhof, G. G., & Adams, J. I. (1968). The ultimate uplift capacity of foundations. *Canadian Geotechnical Journal , 5* (4), 224-244.

Meyerhof, G. (1973). Uplift resistance of inclined anchors and piles. *Proceeding of the 8th International Conference on Soil Mechanics and Foundation Engineering*, (pp. 167-172).

Mitsch, M. P., & Clemence, S. P. (1985). The uplift capacity of helix anchors in sand. (S. Clemence, Ed.) *American Society of Civil Engineers* , 26-47.

Murray, E. J., & Geddes, J. D. (1987). Uplift of anchor plates in sands. *Journal of Geotechnical Engineering , 113* (3), 202-214.

Perko, H. A. (2009). *Helical Piles.* Hoboken, New Jersey, United States of America: John Wiley & Sons, Inc.

Powrie, W. (2004). The application of plasticity and limit equilibrium methods to retaining walls. In W. Powrie, *Soil Mechanics: Concepts and Applications* (2nd Edition ed., pp. 385-400). New York, New York, United States of America: Spon Press.

Rowe, R. K., & Davis, E. H. (1982). The behaviour of anchor plates in sand. *Geotechnique , 32* (1), 25-41.

Saeedy, H. S. (1987). Stability of circular vertical earth anchors. *Candian Geotechnical Journal , 24*, 452-456.

Sakai, T., & Tanaka, T. (1998). Scale effect of a shallow circular anchor in dense sand. *Soils and Foundations , 38* (2).

Salgado, R., Bandini, P., & Karim, A. (2000). Shear Strength and Stiffness of Silty Sand. *Journal of Geotechnical and Geoenvironmental Engineering* , 451-462.

Santamarina, J. C., & Cho, G. C. (2001). Determination of Crictical State Parameters in Sandy Soils-Simple Procedure. *Geotechnical Testing Journal , 24* (2), 185-192.

Sarac, D. Z. (1989). Uplift capacity of shallow buried anchor slabs. *International Conference of Soil Mechanics and Foundation Engineering*, *12*, pp. 1213-1218.

Tufenkjian, M.R., & Yee, E. 2006. Soil Friction Angle and Relative Density of Sand From Minicone Penetration Tests at Shallow Depth. *Report prepared for Ocean Engineering Division, Naval Facilities Engineering Service Center*, Port Hueneme, California, 87 pages, June.

Vesic, A. S. (1971). Breakout Resistance of Objects Embedded in Ocean Bottom. *Soil Mechanics and Foundations Division , 97* (SM9), 1183-1205.

White, D. J., Cheuk, C. Y., & Bolton, M. D. (2008). The uplift resistance of pipes and plate anchors buried in sand. *Geotechnique , 58* (10), 771-779.

Yu, H. S., Salgado, R., & Sloan, S. W. (1998). Limit analysis versus limit equilibrium for slope stability. *Journal of Geotechnical and Geoenvironmental Engineering, 124* (1), 1-11.